0026-895X/97/050741-14$3.00/0

MOLECULAR PHARMACOLOGY, **51:**741–754 (1997).

Expression of Enzymatically Active CYP3A4 by Caco-2 Cells Grown on Extracellular Matrix-Coated Permeable Supports in the Presence of 1α,25-Dihydroxyvitamin D_3

PHYLLISSA SCHMIEDLIN-REN, KENNETH E. THUMMEL, JEANNINE M. FISHER, MARY F. PAINE, KENNETH S. LOWN, and PAUL B. WATKINS

Department of Internal Medicine, University of Michigan Medical Center, Ann Arbor, Michigan 48109 (P.S.-R., K.S.L., P.B.W.), and Department of Pharmaceutics, University of Washington, Seattle, Washington 98195 (K.E.T., J.M.F., M.F.P.)

Received November 6, 1996; Accepted January 24, 1997

SUMMARY

The human colon carcinoma cell line, Caco-2, is widely used as a model for oral absorption of xenobiotics. The usefulness of Caco-2 cells has been limited, however, because they do not express appreciable quantities of CYP3A4, the principle cytochrome P450 present in human small bowel epithelial cells. We report that treatment of Caco-2 cells with 1α,25-dihydroxyvitamin D_3, beginning at confluence, results in a dose- and duration-dependent increase in CYP3A4 mRNA and protein, with little apparent effect on the expression of CYP3A5 or CYP3A7. This treatment also results in increases in NADPH cytochrome P450 reductase and P-glycoprotein (the *MDR1* gene product) but has no detectable effect on expression of CYP1A1, CYP2D6, cytochrome b_5, liver or intestinal fatty acid binding proteins, or villin. Maximal expression of CYP3A4 requires an extracellular matrix on a permeable support and the presence of serum. In the treated cells, the intrinsic formation clearance of 1′-hydroxymidazolam (a reaction characteristically catalyzed by CYP3A enzymes) was estimated to be somewhat lower than that of human jejunal mucosa (1.14 and 3.67 ml/min/g of cells, respectively). The 1′-OH-midazolam/4-OH-midazolam product ratio produced by the cells (~5.3) is comparable to, but somewhat lower than, that observed in human jejunal microsomes (7.4–15.4), which may reflect the presence of CYP3A7 in the Caco-2 cells. 25-Hydroxyvitamin D_3 is less efficacious but reproduces the effects of the dihydroxy compound, whereas unhydroxylated vitamin D is without appreciable effect. These observations, together with the time course of response, suggest that the vitamin D receptor may be involved in CYP3A4 regulation. The culture model we describe should prove useful in defining the role of CYP3A4 in limiting the oral bioavailability of many xenobiotics.

CYP3A4, the principal cytochrome P450 present in human liver (1) and small intestinal epithelial cells (enterocytes) (2, 3), has been implicated in the metabolic elimination of many drugs (4). It has been proposed that first-pass metabolism by intestinal CYP3A4 contributes to the poor oral bioavailability of some of these drugs (5–9). An *in vitro* model capable of predicting the oral bioavailability of CYP3A4 substrates could be very useful during drug development. It has also been proposed that drug interactions involving induction or inhibition of CYP3A4 may be largely occurring at the level of the intestine (3, 6, 7) and not exclusively within the liver, as originally thought. Therefore, an *in vitro* model suitable for studying the role of intestinal CYP3A4 in drug/drug interactions would also be quite valuable.

Caco-2 cells (10), when grown as monolayers on permeable supports, have proved to be useful as a model for studying intestinal permeability (11, 12) and several transport functions, including the transport of some drugs (13–16). However, this human colon carcinoma cell line has thus far fallen short as an ideal model for predicting oral bioavailability or studying drug/drug interactions, in part because of its failure to express substantial amounts of CYP3A4. Although a Caco-2 cell clone was recently shown to express a protein that was detected by an anti-CYP3A antibody (17), the protein did not comigrate with CYP3A4 on polyacrylamide gels. Subsequently, others found that cultures of the parent Caco-2 cell line were capable of metabolizing cyclosporin A to one of the major metabolites known to be produced by CYP3A4; how-

This work was supported by National Institutes of Health Grants GM38149 (P.B.W.) and GM48349 (K.E.T.).

ABBREVIATIONS: DMEM, Dulbecco's modified Eagle's medium; bp, base pair(s); HBSS, Hanks' balanced salt solution; D_3, vitamin D_3; 1α,25-$(OH)_2$-D_3, 1α,25-dihydroxyvitamin D_3; ECL, enhanced chemiluminescence; HEPES, 4-(2-hydroxyethyl)-1-piperazineethanesulfonic acid; IFABP, intestinal fatty acid binding protein; LFABP, liver fatty acid binding protein; *mdr-1*, multidrug resistance gene; MDZ, midazolam; 1′-OH-MDZ, 1′-hydroxymidazolam; 4-OH-MDZ, 4-hydroxymidazolam; PCR, polymerase chain reaction; Pgp, P-glycoprotein; PET, polyethylene terephthalate; PMSF, phenylmethylsulfonyl fluoride; RT, reverse transcription; FBS, fetal bovine serum.

ever, two other metabolites of cyclosporin A characteristically produced by CYP3A4 were not detected (18). The rate of nifedipine oxidation, another CYP3A4-catalyzed reaction, has also been reported to be low in Caco-2 cells (19).

In the current study, in which we added to the culture medium a variety of compounds reported to influence cellular differentiation, we have found that 1α,25-dihydroxyvitamin D_3 results in a dose- and duration-dependent increase in the expression of metabolically active CYP3A4 by confluent Caco-2 cells. This expression is further enhanced when the cells are grown on certain extracellular matrices. The system described should prove useful as a model for assessing the roles of intestinal CYP3A4 in limiting oral bioavailability and in participating in drug/drug interactions.

Experimental Procedures

Materials. Caco-2 cells (American Type Culture Collection HTB37) were obtained from American Type Culture Collection, Rockville, MD. DMEM, other media and supplements, and HBSS were obtained from GIBCO (Grand Island, NY). FBS was obtained from Hyclone (Logan, UT). Millicell CM and PCF culture inserts and the Millicell ERS device were obtained from Millipore (Bedford, MA). Uncoated and commercially coated [unpolymerized collagen type I (200 μg/cm^2), fibrillar collagen (polymerized type I collagen; 200 μg/cm^2), collagen type IV (15 μg/cm^2), laminin (25 μg/cm^2), and Matrigel (2.86 mg/cm^2)] track-etched PET inserts, Matrigel, Growth Factor-Reduced Matrigel (used at 2.86 mg/cm^2), Dispase, ITS, and ITS+ were obtained from Collaborative Biomedical Products (Bedford, MA). 1α,25-$(OH)_2$-D_3, 25-OH-D_3, and unhydroxylated D_3 were obtained from Calbiochem (La Jolla, CA). *N*-Methyl-*N*-(*t*-butyl-dimethylsilyl)trifluoroacetamide was purchased from Pierce Chemical (Rockford, IL). β-Glucuronidase (G-7770) and other chemicals were obtained from Sigma Chemical (St. Louis, MO) and were of tissue culture or molecular biology grades where appropriate. MDZ, $^{15}N_3$-MDZ, 4-OH-MDZ, 1′-OH-MDZ, and 1′-[$^2H_2$]1′-OH-MDZ were gifts from Dr. Bruce Mico (Roche Laboratories, Nutley, NJ). Additional stable isotope-labeled internal standards ($^{15}N_3$-1′-OH-MDZ and $^{15}N_3$-4-OH-MDZ) were generated from an incubation of $^{15}N_3$-MDZ with human liver microsomes. Briefly, human liver microsomes, containing 6 nmol of total cytochrome P450, were incubated with 100 μg of $^{15}N_3$-MDZ and 12 mg of NADPH in 100 mM potassium phosphate buffer, pH 7.4, for 10 min at 37°. The reaction (8 ml final volume) was stopped by the addition of 8 ml of 100 mM Na_2CO_3, pH 12.5. $^{15}N_3$-labeled hydroxy products were extracted twice with 20 ml of ethyl acetate. Solvent was removed under nitrogen. The remaining solid was redissolved in 20 ml of methanol and stored in aliquots at −20°.

Stock solutions of 1α,25-$(OH)_2$-D_3, 25-(OH)-D_3, and D_3 were made in absolute ethanol or dimethylsulfoxide; test and control cultures contained 0.1–0.2% ethanol or 0.2% dimethylsulfoxide. The midazolam stock solution was 4 mM in dimethylsulfoxide.

Cell culture. All cultures were maintained in a humidified 37° incubator with a 5% carbon dioxide in air atmosphere. Caco-2 cells were obtained at passage 19 and grown in plastic tissue culture dishes in a medium consisting of DMEM containing 25 mM glucose and 2 mM L-glutamine and supplemented with 0.1 mM nonessential amino acids, 45 nM DL-α-tocopherol, 100 units/ml sodium penicillin G, and 100 μg/ml streptomycin. Complete growth medium was then prepared by the addition of 20% heat-inactivated FBS. When the cells reached 80% confluence, they were removed using 0.1% trypsin/0.537 mM EDTA, diluted 1:3, and reseeded onto fresh tissue culture dishes.

Clones were prepared from the parent cell line at passage 27 by limiting dilution (i.e., a dilute suspension of passage 27 Caco-2 cells was prepared and distributed into the wells of microtiter plates such that each well was expected to receive 0.5–1 cell; these wells were observed microscopically, and the cells from wells that seemed to contain only a single colony were propagated further in culture). For the experiments described below, the clones were used at passages 9-16, whereas the parent cell line was used at passage 24 or 27.

For our experiments, the cells were seeded at 6×10^5 cells/cm^2 onto the membranes of culture inserts using complete growth medium. The following day, the membranes were washed three times, and fresh medium was added. Subsequent medium changes were at 2–3-day intervals. In all experiments, protein analysis and metabolic activity assay were done from a single 30-mm insert per time point or per culture condition variation. RNA analysis was done from a separate 12- or 10-mm insert. Millicell CM (Teflon membrane; 0.4 μm pore size) culture inserts, which require an extracellular matrix coating for cell adherence, were used primarily. All CM inserts were coated with a dried film of Matrigel according to manufacturer's (Millipore) instructions. Matrigel was thawed on ice, diluted with ice-cold sterile water to 1.35 mg/ml, and dispensed (225 μg/cm^2) into precooled inserts using precooled pipette tips. The inserts were then allowed to dry overnight in a laminar flow hood.

In our initial studies, we found that Caco-2 cells demonstrated a marked tendency to pull away from the perimeter of Matrigel-coated inserts [as previously reported by others using Madin Darby Canine Kidney cells (20)] and form complex structures rather than maintaining a confluent monolayer pattern of growth, thereby making many of the cultures unusable. This was worsened by increasing the amount of Matrigel/cm^2 of surface area of the inserts or using it as a gel instead of a dried film. In a small trial to compare various extracellular matrices, we used commercially coated PET inserts (1 μm pore size). Caco-2 cells grown on Growth Factor-Reduced Matrigel, laminin, collagen type IV, collagen type I, and polymerized collagen type I (fibrillar collagen) demonstrated a monolayer pattern of growth and a more rapid achievement of confluence than did cells grown on Matrigel. On the inserts commercially coated with unpolymerized collagen type I and, to a lesser degree, on the inserts coated with collagen type IV, the Caco-2 cells demonstrated dome formation, indicating that there was impairment of water and electrolyte movement across the membrane. This alone renders the inserts commercially coated with unpolymerized collagen type I and collagen type IV unusable for studies of drug absorption. In an experiment to study the effect of the presence or absence of extracellular matrix, Millicell PCF inserts (polycarbonate membrane; 3.0 μm pore size), which do not require a matrix coating for cell adherence, were used with and without a Matrigel coating.

On achieving confluence (transepithelial resistance of $\geq$250 $\Omega \cdot$cm^2 (21) as measured using a Millicell ERS device), the basic medium was additionally supplemented (to the indicated final concentrations) with sodium selenite (0.1 μM), zinc sulfate (3 μM), and ferrous sulfate (5 μM). Complete differentiation medium was then prepared by the addition of 5% heat-inactivated FBS. Where indicated, the medium of some cultures was additionally supplemented with retinol acetate, menadione sodium bisulfite, δ-aminolevulinic acid, sodium pyruvate, sodium butyrate, vitamin D_2, 1α,25-$(OH)_2$-D_3, 25-(OH)-D_3, or D_3. In another experiment, serum-free differentiation media were compared with the 5% FBS-containing medium. The cells from all experiments were maintained in their respective differentiation media for 2 weeks postconfluence and then used for MDZ metabolism studies and/or harvested for analysis of protein or mRNA.

A separate comparison was made using several different cell culture media as the basic component of the 5% FBS-containing differentiation medium used during the 2 weeks postconfluence. All of the complete differentiation media in this trial were formulated to contain equal amounts of glucose, L-glutamine, selenium, zinc, and vitamin E, and all were supplemented with 0.25 μM 1α,25-$(OH)_2$-D_3. Results showed that CYP3A catalytic activity was greater in cultures grown in DMEM, DMEM/F12 (1:1), or Williams' E based medium than in cultures grown in Iscove's, Iscove's/F12/NCTC135 (5:5:1),

RPMI 1640, McCoy's 5A, Waymouth 752/1, Waymouth with 0.1 mM nonessential amino acids, Medium 199, CMRL 1066, or CMRL/F12 (4:1) based medium (not shown). However, the differences in catalytic activity among cells grown in the various media were < 4-fold. Review of the media components did not reveal any single factor shared by DMEM and Williams' E media that is not also present in one or more of the other media that did not perform as well.

An experiment to determine whether the duration of exposure to 1α,25-(OH)$_2$-D$_3$ could be shortened without diminishing the expression of CYP3A was conducted in such a manner that all cultures were of the same age (2 weeks postconfluence) at the time of harvesting. On reaching confluence, the medium in all cultures was changed from growth medium containing 20% FBS to differentiation medium containing 5% FBS, but 0.25 μM 1α,25-(OH)$_2$-D$_3$ was added at different times postconfluence and continued until the cells of each particular culture were 2 weeks postconfluence. Each time point was represented by duplicate cultures: one for mRNA analysis and another for immunoblots and catalytic activity assay.

For MDZ metabolism studies, the medium was aspirated, and the inserts were washed three times with HBSS. Then, 1.5 ml of fresh complete differentiation medium was placed on each side of the insert, with 4 μM MDZ present in the medium placed on only one side of the monolayer. The incubation media did not contain vitamin D (except that contributed by the 5% FBS).

Preparation for transmission electron microscopy. The medium was aspirated, and the inserts were washed three times with HBSS. The monolayers were fixed in 2% glutaraldehyde/4% tannic acid in cacodylate buffer, postfixed in 1% osmium tetroxide in cacodylate buffer, dehydrated in a graded series of ethanol, and embedded in EPON resin. Sections (70 nm thick) were prepared, poststained sequentially with 4% uranyl acetate and Reynolds lead citrate, and examined with a transmission electron microscope (model CM-10; Philips Electronics Instruments).

Harvesting for immunoblots. The medium was aspirated, and the inserts were washed three times with HBSS containing 15 mM HEPES. Cells grown on Matrigel or Growth Factor-Reduced Matrigel-coated inserts were removed from the membranes using Dispase according to the manufacturer's directions. Then, 5 mM EDTA in normal saline containing 1 mM PMSF and 1 mM benzamidine was added to inhibit further digestion. The cell suspension was transferred to a microcentrifuge tube and pelleted by centrifugation at 325 × *g*. The pellets were washed three times with HBSS containing 15 mM HEPES, 1 mM PMSF, and 1 mM benzamidine. The final pellet was resuspended in a solution of 20% v/v glycerol, 100 mM Tris·HCl, pH 7.4, 10 mM EDTA, 1 mM dithiothreitol, 1 mM PMSF, 1 mM benzamidine, and 100 μg/ml aprotinin and homogenized in a conical ground glass tissue grinder with 20 passes of a ground-glass pestle. The homogenate was subjected to 10 seconds of sonication and was then kept at −80° until analysis.

Cells grown on uncoated inserts or inserts coated with non-Matrigel matrices were harvested by scraping into HBSS containing HEPES and protease inhibitors, washed three times, and then homogenized, sonicated, and frozen as above.

Immunoblots. The protein concentrations of the cell sonicates were measured according to the method of Bradford (22) using bovine serum albumin standards. The sonicates were electrophoresed in polyacrylamide gels containing 0.1% sodium dodecyl sulfate, and the separated proteins were electrophoretically transferred to nitrocellulose. Immunoblot development was performed as previously described (23). CYP3A proteins were detected using a mouse monoclonal antibody named 13–7-10 (24) (a gift from Dr. Pierre Kremers, Université de Liège, Liège, Belgium). This antibody detects all known forms of human CYP3A. CYP3A5 was detected using an immunoadsorbed polyclonal rabbit antibody (25) received as a gift from Dr. Steven A. Wrighton (Eli Lilly, Indianapolis, IN). CYP2D6 was detected using a polyclonal rabbit antibody developed against unique antigenic peptides (26) and obtained as a gift from Dr. Alastair Cribb (Merck Research Laboratories, West Point, PA). CYP1A1 was detected using a polyclonal goat antibody (Gentest, Woburn, MA) developed against rat CYP1A1 and CYP1A2 that has been shown to also detect the human forms of these proteins. Reductase and cytochrome b_5 were detected using polyclonal rabbit antibodies developed against the specific rat proteins that were found to also recognize the human forms of these proteins. Briefly, NADPH cytochrome P450 reductase (reductase) was purified from phenobarbital-induced adult rat liver microsomes as previously described (27). Cytochrome b_5 was purified from adult rat liver according to a method identical to that previously described for the purification of rabbit cytochrome b_5 (28). Rabbit polyclonal antibody was produced against each antigen in female New Zealand White rabbits. Animals received an initial subcutaneous injection (250 μg of reductase or 200 μg of cytochrome b_5) in Freund's complete adjuvant followed by an identical booster dose in Freund's incomplete adjuvant 3 weeks later. Peripheral blood was collected over the next 20 weeks, and serum IgG was isolated as previously described (29). Pgp was detected using a polyclonal rabbit antibody (Oncogene Science, Uniondale, NY). Villin was detected using a mouse monoclonal antibody (Chemicon International, Temecula, CA). IFABP and LFABP were detected using polyclonal rabbit antibodies developed against rat proteins that have been shown to detect the human forms of these proteins (30); these antibodies were received as gifts from Dr. Jeffrey Gordon (Washington University School of Medicine, St. Louis, MO). Secondary antibodies of appropriate specificities conjugated with horseradish peroxidase were obtained commercially (rabbit anti-mouse IgG and goat anti-rabbit IgG/A/M from Zymed Laboratories, San Francisco, CA; mouse anti-goat IgG/A/M from Pierce, Rockford, IL). Binding of secondary antibodies was detected using the ECL reagents and film from Amersham (Arlington Heights, IL).

In some cases, immunoblot protein concentrations were determined by computer-aided densitometry. Optical densities were performed on a Macintosh computer using the public-domain NIH Image program.[1] Individual exposures were scanned into binary images with a ScanJetIIc color scanner (Hewlett Packard, Greeley, CO). An absorbance-concentration standard curve was prepared using the bands from second loaded serial dilutions of purified CYP3A4 protein, and the absorbances of unknowns were converted to quantitative numbers by comparison to this curve. This allowed for correction of the nonlinearity of ECL light output and ECL Hyperfilm.

Harvesting for mRNA analyses; RNA isolation. The medium was aspirated, and the culture inserts were washed three times with HBSS containing 15 mM HEPES. Chomczynski and Sacchi's denaturing solution (31) was applied to the monolayer (333 μl/cm^2 insert membrane surface area). After 5 min, the cell lysate was transferred to a microcentrifuge tube and stored at −80°. The lysate was later thawed quickly at 65°, and total RNA was isolated according to the published protocol (31), adjusting reagent volumes proportionately as appropriate for the initial lysate volume.

mRNA analyses. cDNA was prepared from the total RNA as previously described (32). The polymerase chain reaction was performed on 1 μl of a 1:10 dilution in water of a prepared cDNA. Primer sequences for amplification of CYP3A3, CYP3A4, CYP3A5, and CYP3A7 (product sizes of 619, 382, 350, and 469 bp, respectively) cDNAs were as previously described (33), with the following exceptions: the antisense primer for CYP3A5 was 5′-TTC TGG TTG AAG AAG TCC TTG CGT GTC-3′, and the first sense primer (33) for CYP3A3 was paired with the second antisense primer (33). The primers for *mdr-1* cDNA (34) amplification were 5′-GTC ATT GTG GAG AAA GGA AAT CAT G-3′ and 5′-ATT CCA AGG GCT AGA AAC AAT AGT G-3′, product size of 478 bp. The primers for IFABP cDNA (35) amplification were 5′-AGG AAG CTT GCA GCT CAT GAC AAT TTG AAG-3′ and 5′-AGT ATT CAG TTC GTT TCC ATT GTC TGT CCG-3′, product size of 231 bp. The primers used for villin cDNA (36, 37) amplification were 5′-CAG CTA GTG AAC AAG CCT

[1] Developed at the National Institutes of Health and available on the Internet at *http://rsb.info.nih.gov/nih-image/*

GTA GAG GAG CTC-3′ and 5′-GCC ACA GAA GTT TGT GCT CAT AGG CAC ATC-3′, product size of 303 bp. If *CYP3A5* and *CYP3A3* are organized in the same fashion as *CYP3A4* (38) and *CYP3A7* (39), then all synthetic oligonucleotide primer pairs used spanned at least one intron. PCR mixtures were as previously described (32). Each thermal cycle consisted of 95° for 1 min and then 65° for 1 min 15 sec; after completing all cycles, a 10-min extension step at 65° was performed. PCR products were electrophoresed on agarose gels and stained with ethidium bromide. A reagent control, included in each PCR run, was confirmed to be negative when run on the gel. PCR products were judged to be of the size appropriate for amplification of the specific cDNA by comparison with molecular weight standards included on each gel. The sequence of a PCR product produced from Caco-2 cell cDNA by each primer pair was determined by the method of Sanger *et al.* (40) using the plasmid pCR II (InVitrogen, San Diego, CA) and was confirmed to be consistent with the published specific cDNA sequence.

An internal standard for quantitative competitive PCR (41, 42) of CYP3A4 cDNA was prepared by inserting a 30-bp segment into the cDNA sequence to be amplified. PCR mixtures were prepared by combining serial dilutions of a known amount of the standard cDNA and constant amounts of the unknown cDNA. The two cDNAs were amplified together, and the products were separated on agarose gels. After staining with ethidium bromide, the two bands were quantified densitometrically. An equivalence point (at which the densities of the standard and unknown bands are of equal absorbance) was determined; the concentration of the unknown is equal to that of the standard at the point of equivalence. Evidence supports the assumption that the insertion of the 30-bp segment into the standard does not significantly alter amplification efficiency.[2]

MDZ, 1′-hydroxymidazolam, and 4-hydroxymidazolam assays. Measurement of the rate and extent of MDZ 1′-hydroxylation was used as the principal means to assess CYP3A catalytic activity in Caco-2 cell cultures. All culture samples were analyzed in duplicate, and the mean of the two measurements is reported. For quantification of 1′-OH-MDZ, 0.2–1.0 ml of medium removed from the apical or basolateral compartment of a Caco-2 cell culture was diluted with water to a volume of 1 ml. To this was added 1 ml of 50 mM Na_2CO_3, pH 12.5, and 20 ng of 1′-[$^2H_2$]1′-OH-MDZ internal standard. For the analysis of MDZ, 0.02 ml of culture medium was diluted to a volume of 1 ml. To this was added 1 ml of 50 mM Na_2CO_3, pH 12.5, and 40 ng of $^{15}N_3$-MDZ internal standard. Standards were also prepared in duplicate. Known amounts of MDZ and 1′-OH-MDZ (1–50 ng) were combined with 100 mM potassium phosphate buffer, pH 7.4. To this was added 1 ml of 50 mM Na_2CO_3, pH 12.5, and the appropriate amount of stable isotope-labeled internal standard.

Unknowns and standards were extracted with 5 ml of ethyl acetate, and the upper organic layer was transferred to clean tubes. The solvent was evaporated to dryness under a stream of nitrogen. The remaining solid was reconstituted in 100 μl of derivatizing reagent [10% *N*-methyl-*N*-(*t*-butyldimethylsilyl)trifluoroacetamide in acetonitrile]. Samples were transferred to glass autoinjector vials, sealed, and heated at 80° for 2 hr before analysis by gas chromatography-selective ion mass spectrometry (9).

To determine whether the glucuronide conjugate of 1′-OH-MDZ was formed during Caco-2 cell incubations, 0.25-ml aliquots of apical and basolateral culture medium from cells incubated for 2–24 hr with 4 μM MDZ (administered apically) were diluted to a volume of 0.5 ml and added to 0.5 ml of 100 mM sodium acetate, pH 5.0, containing 200 units of β-glucuronidase. Samples were spiked with 20 ng of 1′-[$^2H_2$]1′-OH-MDZ and incubated at 37° for 24 hr. Each of a complete set of parallel 0.25-ml samples was diluted to a volume of 1 ml and spiked with 20 ng of 1′-[$^2H_2$]1′-OH-MDZ (no glucuronidase treatment). All samples were then alkalinized and processed as above, and the 1′-OH-MDZ concentrations were quantified by mass spectrometry.

[2] K. S. Lown, M. Ghosh, and P. B. Watkins, unpublished observations.

The effect of verapamil on MDZ apical/basolateral distribution and 1′-OH-MDZ formation and distribution in Caco-2 cell cultures was also examined. Verapamil (100 μM) was added to the apical medium of 0.25 μM 1α,25-$(OH)_2$-D_3 treated 2 weeks postconfluent Caco-2 cells simultaneously with apical or basolateral administration of 4 μM MDZ. After incubations of 0–24 hr, both apical and basolateral compartments were sampled for measurement of MDZ and 1′-OH-MDZ concentrations.

In selected cultures, the minor CYP3A metabolite, 4-OH-MDZ, was quantified along with 1′-OH-MDZ after incubations with 4 μM MDZ added to the apical medium. For the assay, base-treated culture medium was spiked with $^{15}N_3$-1′-OH-MDZ and $^{15}N_3$-4-OH-MDZ (~50 ng/10 ng fixed ratio) and processed as described above. Standard curves for both 1′-OH-MDZ (1–50 ng) and 4-OH-MDZ (0.5–25 ng) were also prepared. The only modifications to the mass spectrometric assay involved monitoring molecular ions with m/z 455 and 460 (for unlabeled and $^{15}N_3$-labeled ^{37}Cl isotope of 1′-OH-MDZ, respectively) and base peak fragment ions ($[M\text{-}t\text{-}Bu(CH_3)_2SiOH]^-$) with m/z 323 and 328 (for unlabeled and $^{15}N_3$-labeled ^{37}Cl isotope of 4-OH-MDZ, respectively). 4-OH-MDZ exhibited a slightly shorter gas chromatography column retention time than 1′-OH-MDZ (12.7 versus 14.0 min), under previously defined gas chromatographic conditions (9).

For comparison, 1′-OH/4-OH-MDZ product ratios were also measured in incubations of human jejunal microsomes. Microsomes were prepared from 12 different organ donors, as previously described (8) and stored at −70°. Protein concentrations were determined according to the method of Lowry *et al.* (43) using bovine serum albumin standards. Each preparation was analyzed by immunoblotting for CYP3A4 and CYP3A5 content (29). Six were preselected for determination of the MDZ metabolite ratio, based on the detection of both CYP3A4 and CYP3A5 ($n = 3$) or CYP3A4 only ($n = 3$). Microsomal incubations were carried out in duplicate as previously described (8) using 100–200 μg of microsomal protein, with the final MDZ concentration set at 0, 0.25, 1, 4, or 8 μM. Alkalinized incubation samples were spiked with ~50 ng $^{15}N_3$-1′-OH-MDZ and ~10 ng $^{15}N_3$-4-OH-MDZ (fixed ratio) and processed for mass spectrometric analysis as described above.

Determination of 1′-hydroxymidazolam intrinsic formation clearance. An intrinsic 1′-OH-MDZ formation clearance was determined from the 24-hr time course data for 1′-OH-MDZ formation in confluent cultures dosed apically with 4 μM MDZ. Parent drug and metabolite concentrations measured at 1 and 2 hr after MDZ administration were used for computation. The amount of 1′-OH-MDZ formed during this interval was determined as the sum of metabolite in the apical and basolateral compartments at 2 hr minus the total amount measured at 1 hr. The rate of product formation was normalized for the total mass of Caco-2 cells in each culture insert (an average of 65 mg) measured at the end of the MDZ incubation period (after Dispase digestion, washing, and centrifugation of the cells).

Because the incubation medium contained significant amounts of FBS, the fraction of MDZ bound to culture medium proteins was measured by equilibrium dialysis (8). The unbound concentration of MDZ in the apical and basolateral compartments during cell culture was calculated as the product of the experimentally determined MDZ free fraction and total MDZ concentration. Because MDZ concentrations in the apical and basolateral compartments were not at equilibrium during the 1–2-hr MDZ incubation interval, the intracellular reaction was assumed to be driven by a MDZ concentration that was more closely aligned with the concentration in the basolateral compartment. Thus, the intrinsic 1′-OH-MDZ formation clearance (assuming subsaturating MDZ concentrations) was calculated as the ratio of the 1′-OH-MDZ formation rate and the average (1–2 hr) unbound MDZ concentration in the basolateral compartment. This calculation assumes that any potential MDZ transport mechanism is located in the apical membrane.

For comparison, an intrinsic 1′-OH-MDZ formation clearance was

also determined for eight paired human duodenal and jejunal mucosae. The mucosal mass was removed from ~1-foot sections of duodenum and jejunum and total homogenate and microsomes were prepared, as described above. Protein concentrations for homogenate and microsomes were measured according to the method of Lowry *et al.* (43). The specific CYP3A4 content (pmol/mg of protein) in homogenate and microsomes was measured by immunoblot analysis (29). The total amount of microsomal protein per gram of mucosa was determined from the following relationship:

$$\text{mg of microsomal protein/g of mucosa} = \frac{\text{mg of homogenate protein}}{\text{g of mucosa}} \times \frac{\text{mg of microsomal protein}}{\text{mg of homogenate protein}}$$

where

$$\text{mg of microsomal protein/mg of homogenate protein} = \frac{(\text{pmol of CYP3A4/mg of homogenate protein})}{(\text{pmol of CYP3A4/mg of microsomal protein})}$$

This calculation assumes that CYP3A4 found in mucosal homogenate resides exclusively within the microsomal fraction. The intrinsic 1′-OH-MDZ formation clearance/g of mucosa was calculated as the product of the microsomal intrinsic formation clearance and the computed amount of microsomal protein/g of mucosa.

Results

To obtain genetic homogeneity among the cells to be used in our experiments, five clones were prepared from the parent Caco-2 cell line at passage 27. As judged by relative band intensities of RT-PCR products on ethidium-stained gels, all five of the clones seemed to express greater levels of CYP3A4 mRNA than did the parent cell line (not shown). The clone (no. 5) that seemed to have the highest level of expression of CYP3A4 mRNA was found to have poor growth characteristics. A clone (no. 7) with an intermediate level of CYP3A4 mRNA expression was therefore selected for use in the experiments described below.

To define culture conditions that favored expression of CYP3A4 by Caco-2 cells, RT-PCR was used to assess relative levels of CYP3A4 mRNA in 2-week postconfluent cells that had been grown with or without Matrigel or had been exposed to test compounds added to the differentiation medium beginning at the time of confluence. The achievement of confluence was delayed on the Matrigel-coated inserts (average, ~12–25 days) compared with uncoated polycarbonate inserts (~7 days). However, the levels of CYP3A4 mRNA (as well as villin and IFABP mRNAs) generally seemed to be higher when using Matrigel-coated inserts (not shown), and therefore Matrigel was used in subsequent cultures. Vitamin A (retinol acetate, 0.3 μM), vitamin K (menadione sodium bisulfite, 145 nM), vitamin D$_2$ (ergocalciferol, 0.63 μM), δ-aminolevulinic acid (50–100 μM), sodium butyrate (2 mM, in the presence or absence of vitamin D$_2$), or sodium pyruvate (1 mM) did not seem to enhance CYP3A4 mRNA expression. However, the addition of 1α,25-(OH)$_2$-D$_3$ (1α, 25-dihydroxycholecalciferol, 0.63 μM) to the medium was found to result in a dramatic increase in the expression of CYP3A4 mRNA, and this effect was studied further.

A dose-response experiment was performed with concentrations of 1α,25-(OH)$_2$-D$_3$ that spanned the original 0.63 μM concentration for 2 weeks, administered beginning at the time of confluence. 1α,25-(OH)$_2$-D$_3$ resulted in increased CYP3A4 mRNA expression at all concentrations used (0.05–1.00 μM) (Fig. 1). An attempt was made to quantify the fold increase in CYP3A4 mRNA using serial dilutions of an internal standard for competitive amplification and titration (see Experimental Procedures). Due to the very low levels of CYP3A4 mRNA present in untreated cells, precise quantification of the fold induction was difficult, but it appeared that a 40–80-fold increase had occurred. Expression of the closely related CYP3A7 and CYP3A5 mRNAs (44) also seemed to increase in response to 1α,25-(OH)$_2$-D$_3$, but the increase in CYP3A5 mRNA seemed to be of much lesser magnitude (Fig. 1). The effect of 1α,25-(OH)$_2$-D$_3$ was not a general effect on all mRNAs, however, because the levels of *mdr-1*, IFABP, and villin mRNAs did not seem to increase (Fig. 1). CYP3A3 mRNA was not detected in treated or untreated Caco-2 cells by RT-PCR.[3]

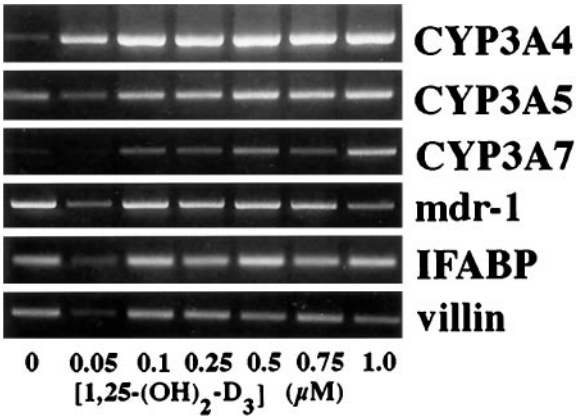

Fig. 1. Changes in Caco-2 cell levels of specific mRNAs in response to treatment with varying doses of 1α,25-(OH)$_2$-D$_3$. Caco-2 cells grown on Matrigel-coated Teflon culture inserts were treated with varying concentrations of 1α,25-(OH)$_2$-D$_3$ for 2 weeks beginning at the time of confluence. Total RNA was then prepared and subjected to RT-PCR using synthetic oligonucleotide primer pairs designed to selectively amplify fragments of the indicated cDNAs. One culture was used for each concentration of 1α,25-(OH)$_2$-D$_3$ (number of PCR cycles: CYP3A4, 36; CYP3A5, 33; CYP3A7, 39; *mdr-1*, 34; IFABP, 32; villin, 27). PCR was done twice with each pair of primers, and the results shown are representative.

The effects of equal concentrations of 1α,25-(OH)$_2$-D$_3$, 25-(OH)-D$_3$, and D$_3$ were then compared in parallel cultures. The CYP3A substrate MDZ (45) (4 μM), was administered apically after 2 weeks of treatment with the vitamin D analogs (i.e., at 2 weeks postconfluence). Treatment with 1α,25-(OH)$_2$-D$_3$ resulted in a dramatic increase in the extent of MDZ metabolism (Fig. 2A; apical concentrations shown). Increases in CYP3A catalytic activity (Fig. 2A) and immunoreactive protein (Fig. 2C) were evident at 0.05 μM 1α,25-(OH)$_2$-D$_3$, and both had plateaued at 0.25–0.5 μM 1α,25-(OH)$_2$-D$_3$. Untreated Caco-2 cells contained ~7.9 pmol of total CYP3A/mg of protein, whereas the maximal expression (at 0.5 μM 1α, 25-(OH)$_2$-D$_3$) corresponded to 20.6 pmol of total CYP3A/mg of cell protein. For comparison, the mean ± standard deviation CYP3A4 content in mucosal homogenates prepared from human duodenum and jejunum was found to be

[3] The existence of CYP3A3 has been questioned (44).

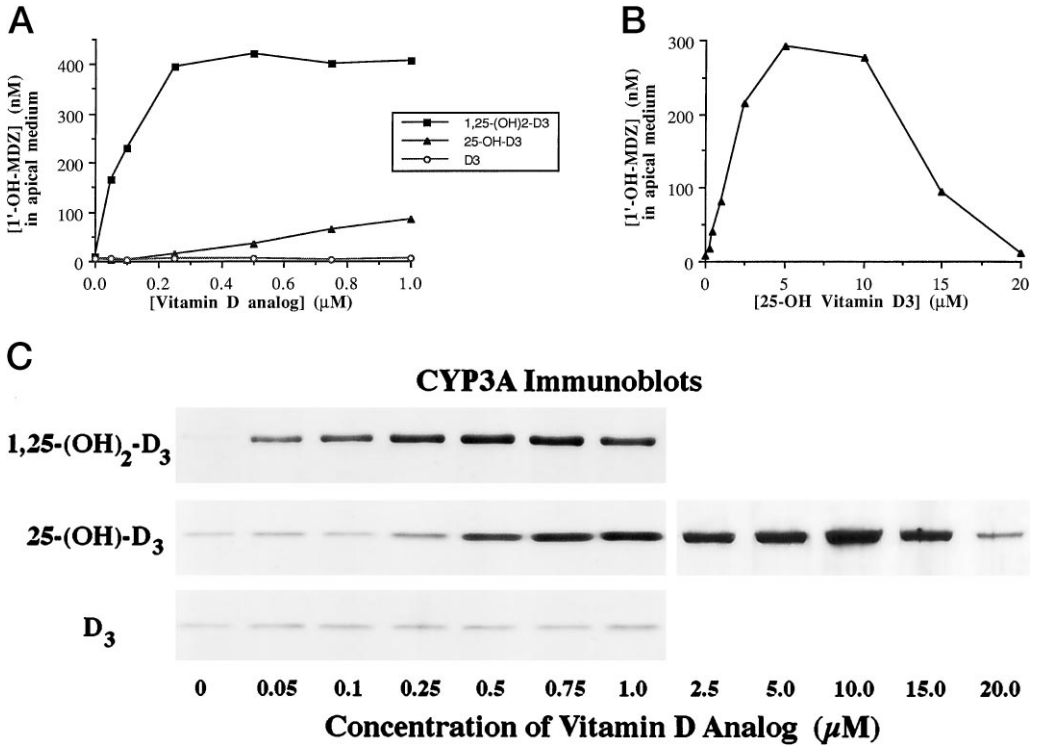

Fig. 2. Changes in Caco-2 cell levels of CYP3A catalytic activity and immunoreactive protein in response to treatment with varying doses of 1α,25-$(OH)_2$-D_3, 25-(OH)-D_3, and D_3. Caco-2 cells grown on Matrigel-coated Teflon culture inserts were treated with varying concentrations of 1α,25-$(OH)_2$-D_3, 25-(OH)-D_3, or D_3 for 2 weeks beginning at the time of confluence. The medium was then replaced with medium not supplemented with vitamin D. MDZ (4 μM) was added to the apical medium. After 6 hr, the apical and basolateral media were removed separately and analyzed for 1′-OH-MDZ concentration. A and B, Data from the apical media. C, Results of immunoblots of cell sonicates (10 μg of protein/lane) developed with a monoclonal antibody that recognizes all known human forms of CYP3A. Each *point* on the graphs represents one culture and corresponds to one *lane* on the immunoblots. A composite blot from two sets of cultures is shown for 25-(OH)-D_3, which required higher doses than did 1α,25-$(OH)_2$-D_3 to achieve a maximal response.

9.2 ± 6.2 and 8.4 ± 5.4 pmol/mg of protein, respectively (Table 1).

In the initial dose-response experiment using 25-(OH)-D_3, CYP3A catalytic activity and immunoreactive protein began to increase at 0.25 μM 25-(OH)-D_3 but the effect had not yet plateaued by 1.0 μM 25-(OH)-D_3, and therefore a dose-response experiment extending to higher concentrations of this agent was performed. CYP3A catalytic activity (Fig. 2B) was maximal at 5 μM 25-(OH)-D_3 and had substantially declined by 15 μM, declining still further at 20 μM 25-(OH)-D_3. Changes in CYP3A immunoreactive protein followed a similar pattern (Fig. 2C). The maximal CYP3A catalytic activity achieved with 25-(OH)-D_3 was not as great as that achieved with 1α,25-$(OH)_2$-D_3. Unhydroxylated D_3 had no effect on immunoreactive CYP3A protein or MDZ metabolism, but concentrations of >1.0 μM were not examined.

TABLE 1

CYP3A content and MDZ hydroxylation activity in human duodenum and jejunum

Total homogenate and microsomes were prepared from mucosal scrapings of paired human duodenum and jejunum from eight different donors. Protein concentration and specific CYP3A content for each tissue fraction was measured as described in Experimental Procedures. Two of eight preparations contained relatively low amounts of CYP3A5 in addition to CYP3A4, which were resolved from one another by SDS-polyacrylamide gel electrophoresis. Microsomes were incubated with varying concentrations of MDZ for determination of K_m and V_{max} parameters for 1′-hydroxylation. The microsomal intrinsic formation clearance was calculated as the ratio of V_{max} to K_m. The mucosal intrinsic formation clearance was calculated from the product of microsomal intrinsic clearance and an experimentally determined concentration of microsomal protein in the total mucosal mass (see text).

	Duodenum	Jejunum
Microsomal CYP3A (pmol/mg of protein)	41.3 ± 30.5	39.7 ± 31.2
Microsomal intrinsic clearance (μl/min/mg of protein)	133.8 ± 109.1	118.3 ± 98.2
Homogenate CYP3A (pmol/mg of protein)	9.2 ± 6.2	8.4 ± 5.4
Mucosal CYP3A (nmol/g of mucosa)	0.89 ± 0.58	0.91 ± 0.61
Mucosal intrinsic clearance (ml/min/g of mucosa)	3.83 ± 3.62	3.67 ± 3.81

Immunoblots showed little change in the level of CYP3A5 in response to 1α,25-$(OH)_2$-D_3 (Fig. 3) or to 25-(OH)-D_3 (not shown). Levels of CYP3A7 could not be assessed because a specific antibody is not available. Levels of CYP1A1 and CYP2D6 did not seem to change in response to 1α,25-$(OH)_2$-D_3 (Fig. 3) or 25-(OH)-D_3 (not shown). The level of reductase seemed to increase in response to concentrations of 1α,25-$(OH)_2$-D_3 of ≥0.05 μM (Fig. 3) and concentrations of 25-(OH)-D_3 of ≥0.5 μM (not shown). An antibody to cytochrome b_5 recognized a protein on immunoblots whose level of expression did not seem to change in response to either 1α,25-$(OH)_2$-D_3 (Fig. 3) or 25-(OH)-D_3 (not shown). The cytochrome b_5 immunoreactive protein in the Caco-2 cells did not comigrate with the major immunoreactive protein present in adult small bowel and liver but did comigrate with a smaller immunoreactive protein present in duodenal homogenate but not detected in human liver microsomes (Fig. 3).

The effect of 1α,25-$(OH)_2$-D_3 and 25-(OH)-D_3 on the expres-

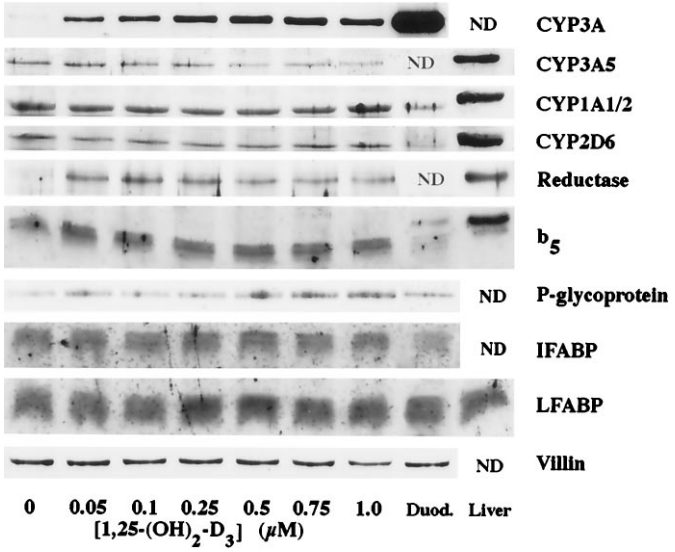

Fig. 3. Caco-2 cell levels of a variety of proteins in response to varying doses of 1α,25-(OH)$_2$-D$_3$. Caco-2 cells grown on Matrigel-coated Teflon culture inserts were treated with varying concentrations of 1α,25-(OH)$_2$-D$_3$ for 2 weeks beginning at the time of confluence. The results of immunoblots of cell sonicates, developed with several antibodies as described in Experimental Procedures, are shown. Each 1α,25-(OH)$_2$-D$_3$ concentration represents one culture. These are the same 1α,25-(OH)$_2$-D$_3$ treated cultures as were used for catalytic activity and immunoblotting in Fig. 2. Caco-2 protein loads were 10 μg for CYP3A, CYP3A5, Pgp, and villin; 25 μg for CYP1A1 and CYP2D6; 40 μg for IFABP and LFABP; and 80 μg for reductase and cytochrome b_5. Human duodenal biopsy homogenate protein loads were 25 μg for CYP3A, Pgp, and villin; 40 μg for CYP1A1; 50 μg for CYP2D6; 60 μg for IFABP and LFABP; and 80 μg for cytochrome b_5. Human liver protein loads were 3 μg for CYP1A2 and CYP2D6, 10 μg for cytochrome b_5, 12 μg for CYP3A5, 25 μg for reductase, and 40 μg for LFABP. Note that liver microsomes were used except for LFABP, for which liver homogenate was used. *ND*, not done. Quantification of the CYP3A immunoreactive bands (*top*) by computer-aided densitometry, using second loaded serial dilutions of purified CYP3A4 protein, revealed that the band from untreated cells (*lane 1*) corresponded to 7.9 pmol of CYP3A/mg of total protein, whereas the band from cells treated with 0.5 μM 1α,25-(OH)$_2$-D$_3$ (*lane 6*) corresponded to 20.6 pmol of CYP3A/mg of total protein. Thus, visual interpretation of immunoblots developed with ECL may overestimate fold increases in levels of expression.

sion of Pgp was examined because many substrates of this transport protein are also CYP3A4 substrates (46, 47). 1α,25-(OH)$_2$-D$_3$ (Fig. 3) and 25-(OH)-D$_3$ (not shown) resulted in a modest increase in levels of immunoreactive Pgp at concentrations of ≥0.5 μM and ≥2.5 μM, respectively.

As control proteins, the responses of IFABP, LFABP, and villin expression to 1α,25-(OH)$_2$-D$_3$ and 25-(OH)-D$_3$ were examined. Neither IFABP nor LFABP showed changes in levels of expression on immunoblots in response to 1α,25-(OH)$_2$-D$_3$ (Fig. 3) or 25-(OH)-D$_3$ (not shown). Levels of villin immunoreactive protein seemed to decrease slightly in response to 1 μM 1α,25-(OH)$_2$-D$_3$ (Fig. 3) or concentrations of 25-(OH)-D$_3$ of ≥10 μM (not shown).

To try to elucidate whether the conditions we had defined for optimal expression of CYP3A4 resulted in a general increase in differentiation, electron micrographs of Caco-2 cells grown in the presence or absence of Matrigel and with or without a 2-week exposure to 0.25 μM 1α,25-(OH)$_2$-D$_3$ were obtained. Ultrastructural differences to indicate differing degrees of differentiation were not detected by an experienced observer (W. O. Dobbins III) who was blinded to the treatments. Measurements of cell height (~16.5 μm) and microvillar height (~1.02 μm) were not clearly affected by the presence or absence of vitamin D or Matrigel. These measurements are similar to those obtained by Wilson *et al.* (17.2 and 0.94 μm), who used uncoated nitrocellulose filters (12), but less than those obtained by Hidalgo *et al.* (29.6 and 1.19 μm), who used collagen type I-coated polycarbonate filters (11). The microvillar height was also less than that reported by Halline *et al.* (1.52 μm) for Caco-2 cells grown on plastic and treated with 0.1 μM 1α,25-(OH)$_2$-D$_3$ in medium containing 20% FBS (48). A representative Caco-2 cell grown on a Matrigel-coated polycarbonate membrane and treated with 1α,25-(OH)$_2$-D$_3$ is shown in Fig. 4.

Because 1α,25-(OH)$_2$-D$_3$ is quite expensive, an experiment was undertaken to determine whether the duration of exposure to 1α,25-(OH)$_2$-D$_3$ could be shortened without diminishing the expression of CYP3A. The experiment was conducted so that all cultures were of the same age (2 weeks postconfluence) at the time of harvesting. An increase in CYP3A4 mRNA was evident after 3–4 hr of exposure to 0.25 μM 1α,25-(OH)$_2$-D$_3$ and, by computer aided densitometry, seemed to plateau at 120 hr (5 days) of exposure to 1α,25-(OH)$_2$-D$_3$ (Fig. 5A). Increased CYP3A protein expression became evident on the immunoblots at 18 hr and continued to rise throughout the remainder of the 2-week experiment (Fig. 5A). MDZ metabolism showed a similar pattern, first becom-

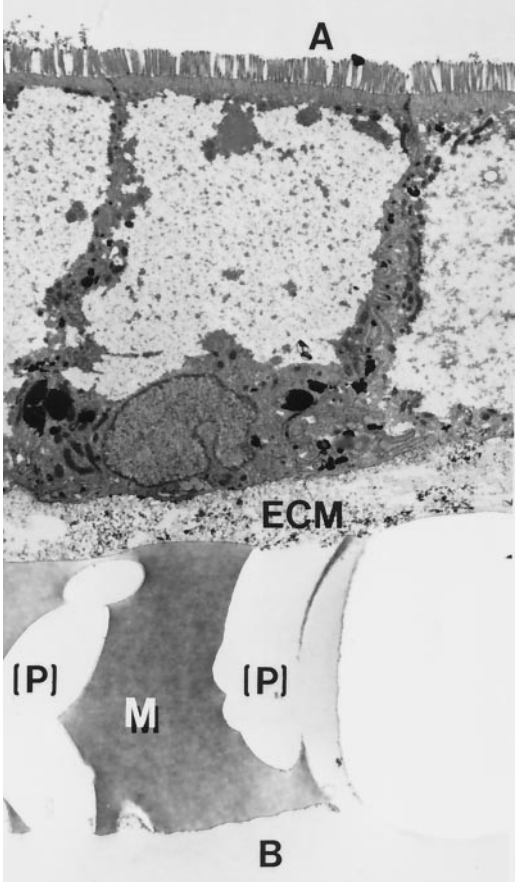

Fig. 4. Electron micrographs of Caco-2 cells grown on a Matrigel-coated polycarbonate culture insert and treated with 0.25 μM 1α,25-(OH)$_2$-D$_3$ for 2 weeks beginning at the time of confluence. Magnification, 10,905×. *A*, apical compartment; *ECM*, Matrigel extracellular matrix; *M*, insert membrane; *P*, pore; *B*, basolateral compartment.

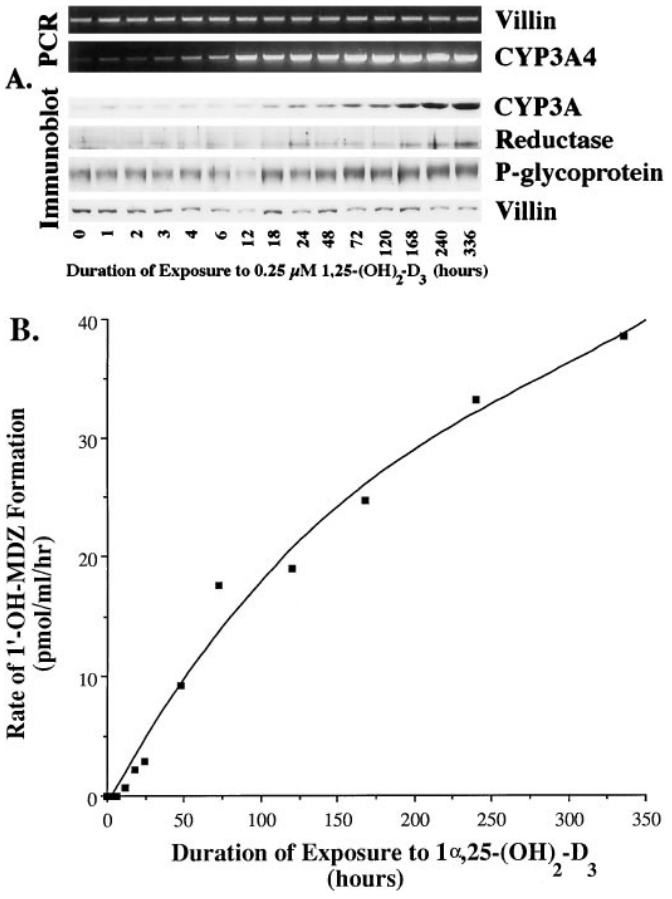

Fig. 5. Duration of exposure to 1α,25-$(OH)_2$-D_3 necessary to achieve increased expression of (A) CYP3A4 mRNA and CYP3A4, reductase, and Pgp immunoreactive proteins and (B) CYP3A catalytic activity by Caco-2 cells. Each time point represents two different cultures: one used for mRNA analysis by RT-PCR, and another used for immunoblots of cell sonicates and catalytic activity. Caco-2 cells were grown on Matrigel-coated Teflon culture inserts and were treated with 0.25 μM 1α,25-$(OH)_2$-D_3 for varying periods. The experiment was conducted such that all cultures were of the same age (2 weeks postconfluence) at the time of harvesting (i.e., on reaching confluence, the medium in all cultures was changed from growth medium containing 20% FBS to differentiation medium containing 5% FBS, but 0.25 μM 1α,25-$(OH)_2$-D_3 was added at different times postconfluence and continued until the cells of each particular culture were 2 weeks postconfluence). The medium was then replaced with medium not supplemented with vitamin D. MDZ (4 μM) was added to the apical medium. After 6 hr, the amount of 1′-OH-MDZ was measured in the combined luminal plus basolateral medium from each culture, and the rate of formation was calculated (numbers of PCR cycles: villin, 27; CYP3A4, 36; immunoblot protein loads: 5 μg for CYP3A, Pgp, villin; 40 μg for reductase).

ing detectable in cultures exposed to 1α,25-$(OH)_2$-D_3 for 12 hr and then continuing to rise throughout the remainder of the 2-week experiment (Fig. 5B). Immunoreactive reductase did not seem to increase until 168 hr (7 days) of exposure to 1α,25-$(OH)_2$-D_3 (Fig. 5A). Immunoreactive Pgp seemed to increase beginning at ~72 hr of exposure to 1α,25-$(OH)_2$-D_3 (Fig. 5A). The levels of villin mRNA and immunoreactive protein did not seem to change over the 2-week course of the experiment (Fig. 5A).

We next undertook time course experiments in which 4 μM MDZ was administered for varying lengths of time to either the apical or basolateral medium of Caco-2 cells cultured on Matrigel and exposed to 1α,25-$(OH)_2$-D_3 for 2 weeks postconfluence. 1′-OH-MDZ (Fig. 6A) became detectable by 1 hr after MDZ administration to either compartment. The rate of 1′-OH-MDZ formation seemed to slow slightly over time but remained roughly constant after 6 hr. At every time point, the concentration of 1′-OH-MDZ was greater in the apical medium than in the basolateral medium (Fig. 6A), even when MDZ had been administered basolaterally. The apical concentration of parent compound after apical administration (Fig. 6B) declined over the first 12 hr, but a stable ~1.4-fold apical to basolateral concentration gradient was then maintained for the remainder of the 24 hr. By 12 hr, the parent compound had also been distributed preferentially to the apical medium after basolateral administration (Fig. 6B).

Aliquots of the apical and basolateral media at various time points after apical administration of MDZ were subjected to treatment with glucuronidase before being assayed for 1′-OH-MDZ. There were no differences between the 1′-OH-MDZ concentrations obtained after glucuronidase treatment (not shown) and the concentrations obtained without hydrolysis, indicating that glucuronidation of 1′-OH-MDZ had not occurred in the Caco-2 cells.

We next examined the effect of adding verapamil (100 μM) to the apical compartment during MDZ metabolism time courses (Fig. 6, C and D). This resulted in a ~90% inhibition of 1′-OH-MDZ formation (Fig. 6C versus 6A), but the apical-to-basolateral concentration gradients of both parent MDZ (Fig. 6D) and 1′-OH metabolite (Fig. 6C) were similar to those seen in the absence of verapamil (Fig. 6, B and A, respectively).

An intrinsic 1′-OH-MDZ formation clearance was calculated, as outlined in Experimental Procedures, from the time course data obtained in the cultures dosed apically with MDZ in the absence of verapamil. The rate of 1′-OH-MDZ formation during the 1–2-hr interval was found to be 75.9 pmol/min/g of cells (Table 2). Under equilibrium dialysis conditions, ~89.8% of MDZ was found to be bound to medium proteins, yielding an unbound fraction of 10.2%. Thus, the total and unbound MDZ concentrations in the basolateral compartment were estimated to be 650 and 66.3 nM, respectively. The intrinsic 1′-OH-MDZ formation clearance under nonsaturating conditions [K_m ~3.4 μM (8)] was estimated to be 1.14 ml/min/g of cells. The mean intrinsic 1′-OH-MDZ formation clearance for eight different human duodenal and jejunal microsomes was found to be 133.8 and 118.3 μl/min/mg of protein, respectively (Table 1). Values for each section of intestine were quite variable, with an interindividual variation of 15- and 20-fold for duodenum and jejunum, respectively. The average microsomal protein content ($\pm$ standard deviation) in duodenal and jejunal mucosa was found to be 25.4 $\pm$ 14.4 and 27.7 $\pm$ 18.7 mg of protein/g of mucosa, respectively. Taking the product of the microsomal intrinsic 1′-OH-MDZ formation clearance and microsomal protein content in duodenal and jejunal mucosa, we arrived at intrinsic clearance values of 3.83 $\pm$ 3.62 and 3.67 $\pm$ 3.81 ml/min/g of mucosa, respectively (Table 1). Thus, the intrinsic 1′-OH-MDZ formation clearance for 1α,25-$(OH)_2$-D_3-pretreated Caco-2 cells compared quite respectably with that for human intestinal mucosa, representing 30% and 31% of the mean intrinsic formation clearance determined for human duodenal and jejunal mucosa, respectively.

All CYP3A isoforms catalyze both the 1′- and 4-hydroxylation of MDZ. Different 1′-OH-MDZ/4-OH-MDZ product ratios

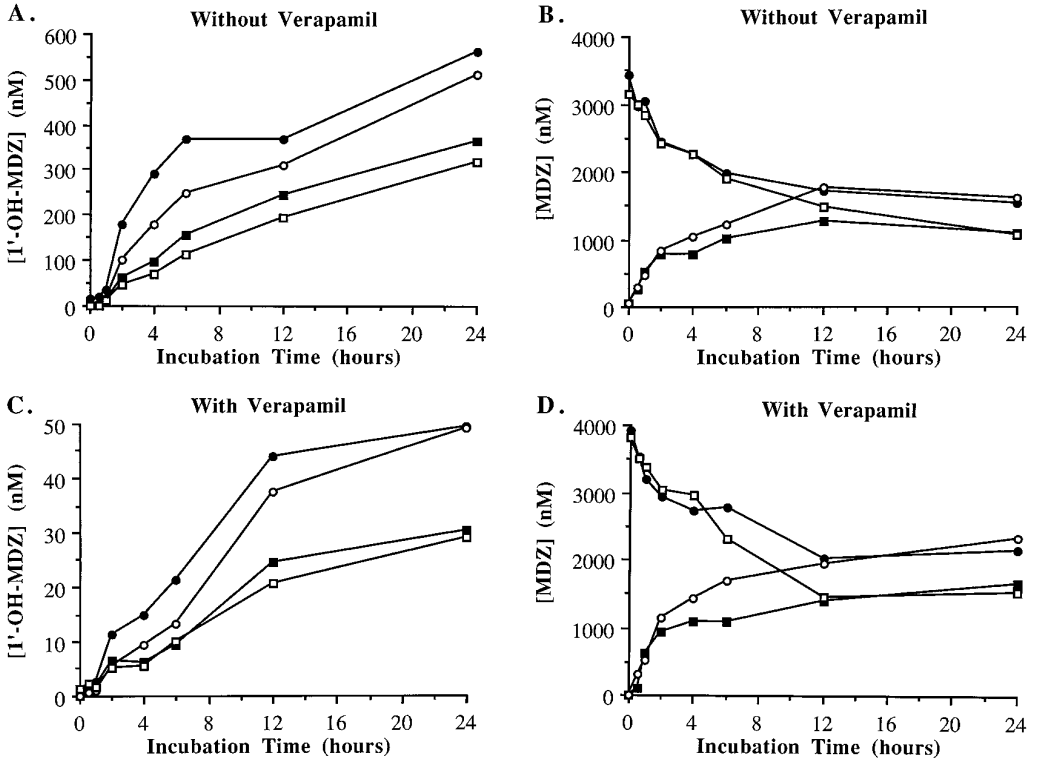

Fig. 6. Time course of MDZ metabolism by Caco-2 cells treated with 1α,25-(OH)$_2$-D$_3$ and the effect of verapamil. Caco-2 cells were grown on Matrigel-coated Teflon culture inserts and treated with 0.25 μM 1α,25-(OH)$_2$-D$_3$ for 2 weeks beginning at the time of confluence. The medium was then replaced with medium not supplemented with vitamin D. MDZ (4 μM) was added to the apical or basolateral medium. C and D, In selected cultures, 100 μM verapamil was applied apically. After incubation, the apical and basolateral media were removed separately and analyzed for concentrations of 1′-OH-MDZ and MDZ. Each *point* (A and C) represents metabolite data from a separate culture, with corresponding parent compound data (B and D). Note the different scales for A and C. ●, Apical medium after apical administration of MDZ. ■, Basolateral medium after apical administration of MDZ. ○, Apical medium after basolateral administration of MDZ. □, Basolateral medium after basolateral administration of MDZ.

TABLE 2

MDZ 1′-hydroxylation kinetics in Caco-2 cell cultures at the 1–2-hr incubation interval

MDZ (4 μM) was added at time zero to the medium in the apical compartment of replicate Caco-2 cell cultures that had been treated with 0.25 μM 1α,25-(OH)$_2$-D$_3$ for 2 weeks after confluence. 1α,25-(OH)$_2$-D$_3$ was not present in the MDZ incubation medium. Both apical and basolateral media were sampled 1 and 2 hr later (from separate cultures) for measurement of MDZ and 1′-OH-MDZ. The unbound fraction of MDZ in culture medium, measured by equilibrium dialysis, was found to be 10.2%. Calculations were performed as described in Experimental Procedures.

1′-OH-MDZ formation rate	75.9 pmol/min/g of cells
Average MDZ concentration	
Basolateral	650 nM
Apical	2740 nM
Unbound MDZ concentration	
Basolateral	66.3 nM
Apical	280 nM
Intrinsic formation clearance	1.14 ml/min/g of cells

are produced by the three known human CYP3A isoforms (CYP3A4, CYP3A5, and CYP3A7) (49). For CYP3A4, metabolism of MDZ at the 1′-position predominates, although hydroxylation at the 4-position is increasingly favored with increasing MDZ concentrations (49). The 1′-OH-MDZ/4-OH-MDZ product formation ratio was measured in selected Caco-2 cell cultures (Table 3) as part of the CYP3A isoform characterization. There was an increase in the product ratio from 3.8 to 5.3 with an increase in duration of treatment (12 versus 336 hr) with 1α,25-(OH)$_2$-D$_3$. Clone 5, which maximally expressed CYP3A immunoreactive protein, had sufficient metabolic activity for measurements to be made in both the 1α,25-(OH)$_2$-D$_3$-treated and untreated states. In the 1α,25-(OH)$_2$-D$_3$-treated culture, the product ratios were 5.4 and 5.2 for apical and basolateral compartments, respectively, whereas in the untreated culture, the product ratios were slightly lower at 4.5 (apical) and 3.6 (basolateral). In cultures of clone 7, which was used for all of the other experiments described here, a product formation ratio of >5 was obtained in 1α,25-(OH)$_2$-D$_3$-treated cells grown on either laminin or Matrigel. In general, product formation ratios determined for intestinal microsomes (Table 4) were higher than those found in Caco-2 cell cultures. For those intestines that contained only CYP3A4, the 1′-OH-MDZ/4-OH-MDZ ratios varied from 7.4 to 9.0 for incubations with 0.25 μM MDZ and from 5.6 to 5.8 for incubations with 8 μM MDZ. As expected, because CYP3A5 gives a higher product ratio than does CYP3A4 (49), higher ratios were generated in incubations with intestinal microsomes containing both CYP3A4 and CYP3A5. Values of 11.1 to 15.4 and 6.7 to 9.7 were measured at 0.25 and 8 μM MDZ, respectively. Thus, product ratios from Caco-2 cell cultures were most similar to those from intestinal microsomes that contained only CYP3A4, although lower than those from intestinal microsome incubations with the most comparable concentrations (0.25–1.0 μM) of MDZ (predicted unbound intracellular concentrations in the Caco-2 cells were ~0.07 μM).

Several other experiments were performed to further characterize our Caco-2 culture model. The use of a particular clone may not be a necessary component to the model because all five of our clones as well as the parent cell line showed increased levels of CYP3A immunoreactive protein after 2 weeks of treatment with 0.25 μM 1α,25-(OH)$_2$-D$_3$ (Fig. 7B). The MDZ 1′-hydroxylation activity of each cell line with and without 1α,25-(OH)$_2$-D$_3$ treatment (Fig. 7A) correlated quite closely with the level of CYP3A immunoreactive protein (p = 0.0003, r = 0.987). There was little variability of reductase expression among the clones and parent cell line when untreated, but there was variable responsiveness to 1α,25-(OH)$_2$-D$_3$; clone 7 had a response similar to that of the parent cell line but greater than that of clone 5 (Fig. 7B). There was

TABLE 3

1′-OH-MDZ/4-hydroxymidazolam formation ratios from incubations of MDZ with cultured Caco-2 cells

Clone 5 is the clone that maximally expresses CYP3A immunoreactive protein, whether treated or untreated with 1α,25-$(OH)_2$-D_3. Clone 7 is the clone that was used for all of the other experiments described.

Cell	Duration of 1α,25-$(OH)_2$-D_3 treatment	Extracellular matrix	Duration of MDZ incubation	1′-OH-MDZ/4-OH-MDZ	
				Apical	Basolateral
	hr		*hr*		
Clone 5					
	336	Matrigel	7.5	5.4	5.2
	Untreated	Matrigel	7.5	4.5	3.6
Clone 7					
	12	Matrigel	6	3.8	N.D.
	120	Matrigel	6	5.1	N.D.
	336	Matrigel	6	5.3	N.D.
	336	laminin	7	5.4	5.2
	336	Matrigel	7	5.3	5.2

N.D., not done.

TABLE 4

1′-OH-MDZ/4-OH-MDZ metabolite concentration ratios from incubations of MDZ with human jejunal microsomes

Microsomes prepared from the jejunum of each of six subjects were selected based on the results of prescreening for the presence of CYP3A4 only or CYP3A4 and CYP3A5. The microsomes from each of these subjects were incubated with varying concentrations of MDZ. Metabolite formation was quantitated as described in Experimental Procedures. The ratios of 1′-OH-MDZ/4-OH-MDZ for all permutations are presented.

	Initial MDZ concentration			
	0.25	1.00	4.00	8.00
		μM		
CYP3A4				
HI-19	7.4	8.1	6.8	5.6
HI-20	9.0	8.9	7.1	5.8
HI-28	8.5	8.6	7.0	5.7
CYP3A4 and CYP3A5				
HI-30	15.4	12.1	12.2	9.7
HI-31	11.2	10.6	8.7	7.0
HI-35	11.1	10.3	8.3	6.7

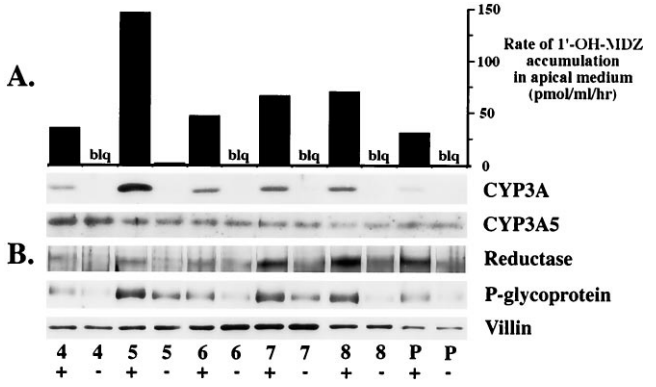

Fig. 7. Comparison of levels of selected immunoreactive proteins and CYP3A catalytic activity in Caco-2 cell clones and the parent cell line and their responses to 1α,25-$(OH)_2$-D_3. All cells were grown on Matrigel-coated Teflon culture inserts. One set of cultures was treated with 0.25 μM 1α,25-$(OH)_2$-D_3 for 2 weeks beginning at the time of confluence (+) while a duplicate set was left untreated (−). The medium was then replaced with medium not supplemented with vitamin D. A, MDZ (4 μM) was added to the apical compartment. After 7.5 hr, the apical and basolateral media were collected separately. The rates of 1′-OH-MDZ accumulation in the apical medium are shown. *blq*, below limits of quantification. B, Immunoblots of sonicates of the cells were developed with antibodies of the indicated specificities. With longer exposures of the film, a CYP3A band was seen with each of the untreated cells (protein loads: 5 μg for CYP3A, CYP3A5, Pgp, villin; 60 μg for reductase). *P*, parent cell line.

considerable variability among the clones with respect to levels of expression of immunoreactive LFABP, with clone 7 being a relatively high expressor (not shown). There was slight variability of Pgp and villin expression among the clones, with clone 7 being a relatively high expressor of both immunoreactive proteins (Fig. 7B). Levels of expression of CYP3A5 (Fig. 7B) and cytochrome b_5, CYP1A1, CYP2D6, and IFABP (not shown) immunoreactive proteins were similar among the clones and the parent cell line.

Matrigel (225 $\mu g/cm^2$) alone did not result in increased expression of CYP3A immunoreactive protein. Nevertheless, although 1α,25-$(OH)_2$-D_3 resulted in increased CYP3A protein and catalytic activity in the absence of Matrigel (Fig. 8A), the increase in CYP3A expression in response to 1α,25-$(OH)_2$-D_3 was clearly enhanced when the Caco-2 cells were grown on Matrigel. The rate of 1′-OH-MDZ formation by Caco-2 cells grown on uncoated culture inserts and treated with 0.25 μM 1α,25-$(OH)_2$-D_3 was only 17% of that of treated cells grown on Matrigel-coated inserts (Fig. 8A). All extracellular matrices were not equal with respect to expression of CYP3A immunoreactive protein and catalytic activity: using commercially coated inserts, unpolymerized collagen type I was associated with relatively low levels of expression and activity, whereas fibrillar collagen (polymerized type I collagen), laminin, Growth Factor-Reduced Matrigel (2.86 mg/cm^2), and (to a lesser extent) collagen type IV were associated with levels of expression and activity similar to that seen with Matrigel (2.86 mg/cm^2) (Fig. 8B).

It also seemed that Caco-2 cell expression of immunoreactive Pgp, although slightly greater with Matrigel than in the absence of a substratum (Fig. 8A), was greater with single component substrata (collagen type I, collagen type IV, or laminin) than with multicomponent substrata (Matrigel or Growth Factor-Reduced Matrigel) (Fig. 8B). Polymerized collagen type I was associated with a level of expression similar to that seen with the multicomponent substrata. These results are similar to those reported for Pgp expression in cultured rat hepatocytes (50).

A Matrigel substratum seemed to increase the level of immunoreactive villin (Fig. 8A). The level of villin expression seemed to be similar among cells grown on all of the extracellular matrices examined (Fig. 8B). The histological ap-

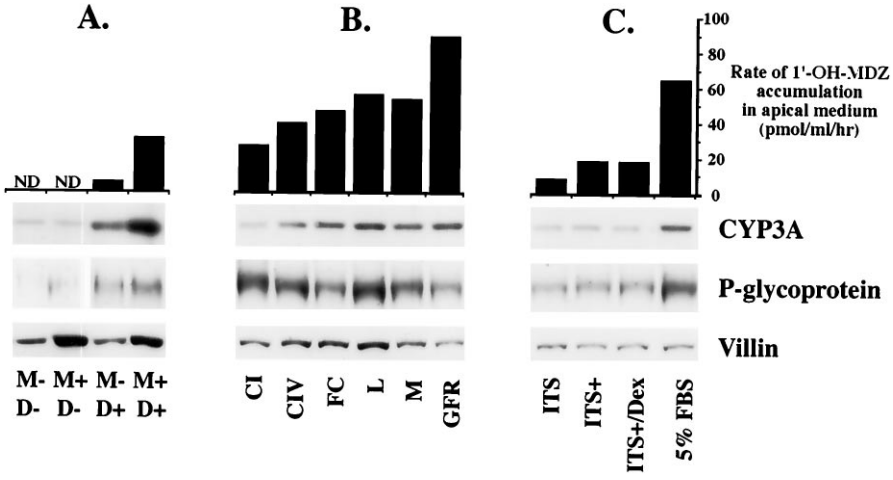

Fig. 8. Effects of extracellular matrices and FBS on the increase in CYP3A in response to 1α,25-(OH)$_2$-D$_3$. At 2 weeks postconfluence, 1α,25-(OH)$_2$-D$_3$ was removed, if present, and the cells were incubated with 4 μM MDZ added to the apical medium. After incubations of 4.25–7 hr (uniform duration within each group), the apical and basolateral media were collected. *Top*, rates of 1′-OH-MDZ accumulation in the apical medium are shown. ND, not done. *Bottom*, immunoblots are of 5-μg loads of cell sonicates developed with antibodies of the indicated specificities. A, Contribution of Matrigel. Caco-2 cells were grown on polycarbonate culture inserts (+*M*) with or (−*M*) without Matrigel. Selected cultures (+*D*) were treated with 0.25 μM 1α,25-(OH)$_2$-D$_3$ for 2 weeks beginning at the time of confluence while duplicate cultures were left untreated (−*D*). (Note that, in the case of Pgp, the first pair of lanes is from a different gel than the second pair of lanes, and therefore direct comparisons can only be made within each pair and not between the pairs of immunoreactive bands.) B, Comparison of extracellular matrices. Caco-2 cells were grown on PET culture inserts commercially coated with several different extracellular matrices [*CI*, unpolymerized collagen type I; *FC*, fibrillar collagen (polymerized type I collagen); *CIV*, collagen type IV; *L*, laminin; *M*, Matrigel] as well as inserts that we coated with Growth Factor-Reduced Matrigel (*GFR*) (see Experimental Procedures for matrix application densities). Note that the growth factor-reduced matrix formed a 1–2-mm-thick gel. All cultures were treated with 0.25 μM 1α,25-(OH)$_2$-D$_3$ for 2 weeks beginning at the time of confluence. C, Contribution of FBS. Caco-2 cells were grown on Matrigel-coated Teflon culture inserts and treated with 0.25 μM 1α,25-(OH)$_2$-D$_3$ in the presence or absence of 5% FBS for 2 weeks beginning at the time of confluence. The serum-free medium was supplemented with ITS (final concentrations: 5 μg/liter selenous acid, 5 mg/liter insulin and transferrin), ITS+ (final concentrations: 6.2 μg/liter selenous acid, 6.2 mg/liter insulin and transferrin, 1.25 g/liter bovine serum albumin, 5.35 mg/liter linoleic acid), or ITS+ with 100 nM dexamethasone (*Dex*).

pearance by light microscopic examination of hematoxylin and eosin-stained sections of formalin-fixed and paraffin-embedded monolayers was similar among Caco-2 cells grown on all of the matrices examined.

Because drugs vary in their degree of protein binding, it would be desirable to be able to eliminate serum from the medium and manipulate the concentration of albumin or other proteins in a model to study the oral bioavailability of drugs. Therefore, responsiveness of CYP3A expression to 1α,25-(OH)$_2$-D$_3$ was compared in Caco-2 cells grown on Matrigel in the presence or absence of 5% FBS for the 2-week postconfluence period. The level of expression of CYP3A immunoreactive protein (Fig. 8C, *bottom*) was similar among the three serum-free cultures but much lower than that achieved with 5% FBS. CYP3A catalytic activity in the serum free cultures was only 30% of that obtained in the presence of 5% FBS (Fig. 8C, *top*). Immunoreactive Pgp also seemed to be diminished in the absence of FBS (Fig. 8C), whereas villin expression seemed to be unaffected. Levels of expression of immunoreactive reductase, cytochrome b_5, IFABP, and LFABP also did not seem to be influenced by the removal of serum (not shown).

It was possible that FBS was functioning to prevent toxicity of 1α,25-(OH)$_2$-D$_3$ by limiting its free concentration, since at the highest concentrations used, both 1α,25-(OH)$_2$-D$_3$ and 25-(OH)-D$_3$ were associated with lower levels of expression of CYP3A4 (Figs. 2C and 3) and villin (Fig. 3). However, lower concentrations of 1α,25-(OH)$_2$-D$_3$ (0.025 nM to 0.1 μM) under serum-free conditions (not shown) failed to significantly increase expression of CYP3A4.

Discussion

We determined conditions under which Caco-2 cells reliably express catalytically active CYP3A4 at levels that seem to be comparable to levels present in mature enterocytes. There seems to be three key components of this system: an extracellular matrix (on a permeable support with low nonspecific binding properties), serum, and exposure to 1α,25-(OH)$_2$-D$_3$ for a 2-week period beginning at the time of confluence. The conclusion that CYP3A4 was the predominant CYP3A isoform upregulated is supported by several observations. First, CYP3A4 mRNA demonstrated a more marked increase in response to 1α,25-(OH)$_2$-D$_3$ than did CYP3A5 mRNA (Fig. 1). Immunoblots clearly demonstrated that CYP3A5, which was present in untreated Caco-2 cells, was not substantially increased (Figs. 3 and 7). CYP3A7 mRNA also seemed to increase. A CYP3A7-specific antibody is not available, so it was not possible to directly assess levels of this protein. However, the presence of catalytically active CYP3A7 in our cells may be suggested by our MDZ metabolite measurements. In incubations with MDZ, CYP3A7 has been reported to generate more 4-OH-MDZ than 1′-OH-MDZ (49), resulting in a 1′-OH-MDZ/4-OH-MDZ product ratio that is less than unity. The ratios we observed (in the range of 5) were lower than would be anticipated from the presence of CYP3A4 and CYP3A5 alone (Table 4) and could be explained by the presence of relatively small amounts of CYP3A7. The increase in the product ratio from 3.8 in the cells treated with 1α,25-(OH)$_2$-D$_3$ for 12 hr to a product ratio of >5 with prolonged (≥120 hr) treatment suggests that CYP3A7 comprised a smaller proportion of the total CYP3A present in

treated compared with untreated cells. Up-regulation of CYP3A4, therefore, seems to predominate.

In addition to CYP3A4, reductase, and Pgp, the levels of certain other proteins seemed to be improved by our culture system. We found immunoreactive CYP1A1 protein to be detectable in uninduced Caco-2 cells, whereas others have found CYP1A1 expression by Caco-2 cells (grown on plastic) to require treatment with inducers (51). CYP2D6 immunoreactive protein expression also seemed to be improved over that reported by others in Caco-2 cells (51). IFABP mRNA and immunoreactive protein were also readily detected in our Caco-2 cells. In contrast, others have been unable to detect either IFABP mRNA by Northern blotting (35, 52) or IFABP immunoreactive protein (52) in Caco-2 cells. We assume that the expression of CYP1A1, CYP2D6, and IFABP resulted from our culture conditions, rather than genetic differences among Caco-2 cells, because the expression of these proteins was comparable in all of our clones as well as in the parent cell line.

Vitamin D (53, 54), extracellular matrix (55, 56), and permeable supports (57) have each been shown to promote differentiation in cell culture systems. Although we could detect no morphological evidence of enhanced differentiation (Fig. 4), it seems likely that improved differentiation accounts for at least some of our observations. However, the dramatic effect of 1α,25-$(OH)_2$-D_3 on CYP3A4 expression seems unlikely to have resulted from improved differentiation alone.

Many of the actions of 1α,25-$(OH)_2$-D_3 (reviewed in Refs. 53 and 54) are mediated by the binding of 1α,25-$(OH)_2$-D_3 to an intracellular vitamin D receptor [known to be present in Caco-2 cells (58)], which is thereby enabled to bind to vitamin D responsive elements in various genes, resulting in their up- or down-regulation. The relative responsiveness of CYP3A4 expression in the Caco-2 cells to 1α,25-$(OH)_2$-D_3, 25-(OH)-D_3, or unhydroxylated D_3 or vitamin D_2 correlates with the relative binding affinities of these compounds to the vitamin D receptor (58). Also, the time between initiation of treatment with 1α,25-$(OH)_2$-D_3 and detectable increase in CYP3A4 mRNA (3–4 hr; Fig. 5A) would be consistent with transcriptional activation. These findings make it likely that the effects of vitamin D on CYP3A4 expression that we observed were mediated through ligand interactions with the receptor.

The nucleotide sequences of several vitamin D-responsive elements in human genes have been published (59–63). None of these sequences were found in a search of the 5′-flanking region of the *CYP3A4* gene (Ref. 38, GenBank D11131). However, Huss *et al.* (64) recently reported that an 84-bp fragment of the 5′ regulatory region of the rat *CYP3A23* gene, which is necessary for both maintenance of basal transcriptional activity and glucocorticoid-mediated increases in transcription, contains an imperfect repeat (5′-AACTCAAAGGAGGTCA-3′). This sequence is homologous to a class of steroid response elements that bind the estrogen receptor family and did not bind the glucocorticoid receptor (64). Of relevance to our observations, when these investigators mutated just two nucleotides and deleted one of the nucleotides separating the repeats (5′-AGGTCA__AGGAGGTCA-3′), they created a typical vitamin D response element and improved the glucocorticoid responsiveness of their construct nearly 2-fold. It should also be noted that the 19-nucleotide sequence implicated in rifampin-mediated transcription of the *CYP3A4* gene (65) contains the identical imperfect repeat described by Huss *et al.* (64). In aggregate, these and our observations suggest that this regulatory element may bind the vitamin D receptor or some other member (known or orphan) of this class of hormone receptors and that this receptor may be involved in transcriptional activation of CYP3A genes by xenobiotics. Because maximal responsiveness to 1α,25-$(OH)_2$-D_3 required the presence of extracellular matrix (Fig. 8A), we postulate that extracellular matrix may result in increased expression of the relevant receptor, thereby increasing vitamin D responsiveness.

The increase in reductase expression after 1α,25-$(OH)_2$-D_3 treatment was very delayed (7–10 days; Fig. 5A), and we postulate that its increased expression may be in response to another induced protein, perhaps CYP3A4, rather than in direct response to 1α,25-$(OH)_2$-D_3. Interestingly, we have found that CYP3A4 and reductase levels in human small intestine decrease in parallel in a proximal to distal direction.[4] The increase in Pgp expression in response to 1α,25-$(OH)_2$-D_3 may be by a post-transcriptional mechanism because we could detect no change in mRNA levels (Fig. 1).

The potential utility of our model was demonstrated by MDZ time course experiments (Fig. 6). MDZ was chosen as the probe drug because it is a well characterized CYP3A4 substrate and because it has been shown to undergo extensive first-pass metabolism in the intestine after oral administration (9). In our Caco-2 cell cultures, catalytic activity was maintained for ≥24 hr after administration of MDZ. Preferential distribution of both MDZ (Fig. 6, B and D) and its 1′-hydroxy metabolite (Fig. 6, A and C) to the apical compartment was observed, even after basolateral administration of the MDZ, indicating that both the parent and metabolite are actively transported in the apical direction. The apical-to-basolateral concentration gradient of the metabolite (1.55-fold) was comparable to, or perhaps slightly greater than, that of the parent compound (1.40-fold).

Because many substrates for CYP3A4 also seem to be substrates for Pgp (46, 47), it seemed likely that Pgp might be responsible for the concentration gradients of MDZ and 1′-OH-MDZ that we observed. We therefore anticipated that the gradients would be diminished in the presence of the known Pgp inhibitor verapamil [K_i =17 μM, determined in Caco-2 cell monolayers (14)]. However, verapamil (100 μM) had no detectable effect on the concentration gradients generated for either parent compound or metabolite, suggesting that Pgp may not be involved. Although more complete studies would be necessary to confidently exclude a role for Pgp, secretory efflux of xenobiotics not mediated by Pgp seems to occur in Caco-2 cells (67). In contrast to the lack of change in concentration gradients, the rate of metabolism of MDZ was reduced by ~90% in the presence of verapamil (Fig. 6C versus 6A). Because verapamil is a substrate for CYP3A4, the decreased metabolism we observed presumably resulted from competitive inhibition of the enzyme [K_i = 23.5 μM, determined in cultured hepatocytes (68)].

It should be noted that exposure to 1α,25-$(OH)_2$-D_3 resulted in far greater increases in CYP3A4 catalytic activity (>50-fold, Figs. 2A and 5B) than in CYP3A immunoreactive protein (~3-fold). This suggests that the CYP3A enzymes present in untreated cells are largely inactive and that factors other than the increase in CYP3A protein contribute to the increases in catalytic activity we observed. One impor-

[4] M. F. Paine, M. Khalighi, J. M. Fisher, D. D. Shen, K. L. Kunze, C. L. Marsh, J. D. Perkins, K. E. Thummel. Characterization of inter- and intra-intestinal differences in human CYP3A-dependent metabolism. Manuscript in preparation.

tant factor may be the increase in reductase that was also observed during treatment (Figs. 3 and 7). However, it is unlikely that the increase in this essential coenzyme alone is responsible because the rapid rise in catalytic activity (Fig. 5B) seems to occur before the increase in reductase protein (Fig. 5A). It seems likely that other processes essential for optimal catalytic activity (e.g., heme incorporation into apoprotein) are also improved by our culture conditions.

The Caco-2 cells did not seem to produce the glucuronide of 1′-OH-MDZ, which is a major metabolite found in blood and urine of patients administered MDZ intravenously or orally (9). However, it has recently been demonstrated that 1′-OH-MDZ glucuronidation occurs primarily in the liver and not in the intestine *in vivo* (9). The absence of this glucuronidation in our system is therefore expected.

There are some potential limitations to our model. The presence of 5% FBS in the medium was found to be required for a maximal increase in CYP3A4 expression (Fig. 8C), and this could confound metabolism and transport studies due to protein binding. However, it should be possible to perform drug metabolism studies under serum-free conditions by withdrawing serum for a limited (e.g., 6–24 hr) study period after maximization of CYP3A4 expression by a 2-week treatment with 1α,25-(OH)$_2$-D$_3$ or 25-(OH)-D$_3$. In addition, the level of CYP3A catalytic activity in the Caco-2 cells is not as great as that estimated in enterocytes *in vivo*. The specific CYP3A content in 1α,25-(OH)$_2$-D$_3$ treated Caco-2 cell cultures was higher than the mean CYP3A content in duodenal and jejunal mucosal homogenate (20.6 pmol/mg of Caco-2 cell protein versus 9.2 and 8.4 pmol/mg of duodenal and jejunal homogenate protein, respectively), whereas the mean intrinsic 1′-OH MDZ formation clearance for Caco-2 cells was only 30% and 31% of the intrinsic formation clearances for duodenal and jejunal mucosae, respectively (1.14 ml/min/g of Caco-2 cells versus 3.83 and 3.67 ml/min/g of mucosa). This may relate to the possible lack of expression of intact cytochrome b_5, a coenzyme required for full activity by CYP3A4 in many of the reactions it catalyzes (69, 70). However, because a plateau was not observed with increasing duration of 1α,25-(OH)$_2$-D$_3$ treatment up to 2 weeks (Fig. 5), it is possible that continuing treatment beyond that time may result in further increases in CYP3A4 catalytic activity.

As a final note, we have previously shown that there are large interindividual differences in the levels of CYP3A4 in small intestinal mucosa (23). Based on our observations in Caco-2 cells, it is possible that interindividual differences in dietary intake or production of vitamin D analogs may partially account for variation in CYP3A4 expression. However, it should be noted that the doses of 1α,25-(OH)$_2$-D$_3$ (0.25 μM) and 25-(OH)-D$_3$ (10 μM) required to obtain maximal expression of CYP3A4 greatly exceed the levels found in normal human serum (≤144 and ≤0.2 pM, respectively).

In summary, we developed an *in vitro* model that we believe represents a major advance in the study of the roles of intestinal CYP3A4 in determining oral bioavailability and in drug/drug interactions. In our system, Caco-2 cells express metabolically active CYP3A4 at levels that seem to be comparable to levels present in small intestinal enterocytes. Future studies will address the mechanism of the effects of 1α,25-(OH)$_2$-D$_3$, whether this culture system results in Caco-2 cells capable of responding to known inducers of CYP3A4, and the utility of the system in drug development.

References

1. Shimada, T., and F. P. Guengerich. Evidence for cytochrome P450NF, the nifedipine oxidase, being the principal enzyme involved in the bioactivation of aflatoxins in human liver. *Proc. Natl. Acad. Sci. USA* **86:**462–465 (1989).
2. Watkins, P. B., S. A. Wrighton, E. G. Schuetz, D. T. Molowa, and P. S. Guzelian. Identification of glucocorticoid-inducible cytochromes P-450 in the intestinal mucosa of rats and man. *J. Clin. Invest.* **80**:1029–1036 (1987).
3. Kolars, J. C., P. Schmiedlin-Ren, J. D. Schuetz, C. Fang, and P. B. Watkins. Identification of rifampin-inducible P450IIIA4 (CYP3A4) in human small bowel enterocytes. *J. Clin. Invest.* **90**:1871–1878 (1992).
4. Guengerich, F. P. Catalytic selectivity of human cytochrome P450 enzymes: relevance to drug metabolism and toxicity. *Toxicol. Lett.* **70:**133–138 (1994).
5. Kolars, J. C., W. M. Awni, R. M. Merion, and P. B. Watkins. First-pass metabolism of cyclosporin by the gut. *Lancet* **338:**1488–1490 (1991).
6. Hebert, M. F., J. P. Roberts, T. Prueksaritanont, and L. Z. Benet. Bioavailability of cyclosporine with concomitant rifampin administration is markedly less than predicted by hepatic enzyme induction. *Clin. Pharmacol. Ther.* **52:**453–457 (1992).
7. Gomez, D. Y., V. J. Wacher, S. J. Tomlanovich, M. F. Hebert, and L. Z. Benet. The effects of ketoconazole on the intestinal metabolism and bioavailability of cyclosporine. *Clin. Pharmacol. Ther.* **58:**15–19 (1995).
8. Thummel, K. E., D. O'Shea, M. F. Paine, D. D. Shen, K. L. Kunze, J. D. Perkins, and G. R. Wilkinson. Oral first-pass elimination of midazolam involves both gastrointestinal and hepatic CYP3A-mediated metabolism. *Clin. Pharmacol. Ther.* **59:**491–502 (1996).
9. Paine, M. F., D. D. Shen, K. L. Kunze, J. D. Perkins, C. L. Marsh, J. P. McVicar, D. M. Barr, B. S. Gillies, and K. E. Thummel. First-pass metabolism of midazolam by the human intestine. *Clin. Pharmacol. Ther.* **60:** 14–24 (1996).
10. Pinto, M., S. Rubine-Leon, M.-D. Appay, M. Kedinger, N. Triadou, E. Dussaulx, B. LaCroix, P. Simon-Assmann, K. Haffen, J. Fogh, and A. Zweibaum. Enterocyte-like differentiation and polarization of the human colon carcinoma cell line Caco-2 in culture. *Biol. Cell* **47:**323–330 (1983).
11. Hidalgo, I. J., T. J. Raub, and R. T. Borchardt. Characterization of the human colon carcinoma cell line (Caco-2) as a model system for intestinal epithelial permeability. *Gastroenterology* **96:**736–749 (1989).
12. Wilson, G., I. F. Hassan, C. J. Dix, I. Williamson, R. Shah, M. Mackay, and P. Artursson. Transport and permeability properties of human Caco-2 cells: an in vitro model of the intestinal epithelial cell barrier. *J. Control. Rel.* **11:**25–40 (1990).
13. Karlsson, J., S.-M. Kuo, J. Ziemniak, and P. Artursson. Transport of celiprolol across human intestinal epithelial (Caco-2) cells: mediation of secretion by multiple transporters including P-glycoprotein. *Br. J. Pharmacol.* **110:**1009–1016 (1993).
14. Hunter, J., M. A. Jepson, T. Tsuruo, N. L. Simmons, and B. H. Hirst. Functional expression of P-glycoprotein in apical membranes of human intestinal Caco-2 cells. *J. Biol. Chem.* **268:**14991–14997 (1993).
15. Augustijns, P. F., T. P. Bradshaw, L.-S. L. Gan, R. W. Hendren, and D. R. Thakker. Evidence for a polarized efflux system in Caco-2 cells capable of modulating cyclosporin A transport. *Biochem. Biophys. Res. Commun.* **197:**360–365 (1993).
16. Thwaites, D. T., M. Cavet, B. H. Hirst, and N. L. Simmons. Angiotensin-converting enzyme (ACE) inhibitor transport in human intestinal epithelial (Caco-2) cells. *Br. J. Pharmacol.* **114:**981–986 (1995).
17. Carriere, V., T. Lesuffleur, A. Barbat, M. Rousset, E. Dussaulx, P. Costet, I. deWaziers, P. Beaune, and A. Zweibaum. Expression of cytochrome P-450 3A in HT29-MTX cells and Caco-2 clone TC7 [Published erratum in *FEBS Lett.* **362:**99 (1995).] *FEBS Lett.* **355:**247–250 (1994).
18. Gan, L.-S. L., M. A. Moseley, B. Khosla, P. F. Augustijns, T. P. Bradshaw, R. W. Hendren, and D. R. Thakker. CYP3A-like cytochrome P450-mediated metabolism and polarized efflux of cyclosporin A in Caco-2 cells. *Drug Metab. Dispos.* **24:**344–349 (1996).
19. Boulenc, X., M. Bourrie, I. Fabre, C. Roque, H. Joyeux, Y. Berger, and G. Fabre. Regulation of cytochrome P450IA1 gene expression in a human intestinal cell line, Caco-2. *J. Pharmacol. Exp. Ther.* **263:**1471–1478 (1992).
20. Pitt, A. M., J. E. Gabriels, F. Badmington, J. McDowell, L. Gonzales, and M. E. Waugh. Cell culture on a microscopically transparent microporous membrane. *Biotechniques* **5:**162–171 (1987).
21. Traber, M. G., H. J. Kayden, and M. J. Rindler. Polarized secretion of newly synthesized lipoproteins by the Caco-2 human intestinal cell line. *J. Lipid Res.* **28:**1350–1363 (1987).
22. Bradford, M. M. A rapid and sensitive method for the quantitation of microgram quantities of protein utilizing the principle of protein-dye binding. *Anal. Biochem.* **72:**248–254 (1976).
23. Lown, K. S., J. C. Kolars, K. E. Thummel, J. L. Barnett, K. L. Kunze, S. A. Wrighton, and P. B. Watkins. Interpatient heterogeneity in expression of CYP3A4 and CYP3A5 in small bowel. *Drug Metab. Dispos.* **22:**947–955 (1994) [published erratum appears in *Drug Metab. Dispos.* **23(3)** (1995).].
24. Beaune, P., P. Kremers, F. Letawe-Goujon, and J. E. Gielen. Monoclonal antibodies against human liver cytochrome P-450. *Biochem. Pharmacol.* **34:**3547–3552 (1985).
25. Wrighton, S. A., W. R. Brian, M.-A. Sari, M. Iwasaki, F. P. Guengerich, J.

L. Raucy, D. T. Molowa, and M. Vandenbranden. Studies on the expression and metabolic capabilities of human liver cytochrome P450IIIA5 (HLp3). *Mol. Pharmacol.* **38:**207–213 (1990).
26. Cribb, A., C. Nuss, and R. Wang. Antipeptide antibodies against overlapping sequences differentially inhibit human CYP2D6. *Drug Metab. Dispos.* **23:**671–675 (1995).
27. Lee, C. A., K. E. Thummel, T. F. Kalhorn, S. D. Nelson, and J. T. Slattery. Inhibition and activation of acetaminophen reactive metabolite formation by caffeine: roles of cytochromes P-450 IA1 and IIIA2. *Drug Metab. Dispos.* **19:**348–353 (1991).
28. Thummel, K. E., C. A. Lee, K. L. Kunze, S. D. Nelson, and J. T. Slattery. Oxidation of acetaminophen to N-acetyl-p-aminobenzoquinone imine by human CYP3A4. *Biochem. Pharmacol.* **45:**1563–1569 (1993).
29. Kharasch, E. D., and K. E. Thummel. Human alfentanil metabolism by cytochrome P450 3A3/4. An explanation for the interindividual variability in alfentanil clearance? *Anesth. Analg.* **76:**1033–1039 (1993).
30. Carroll, S. L., K. A. Roth, and J. I. Gordon. Liver fatty acid-binding protein: a cellular marker for studying cellular differentiation in gut epithelial neoplasms. *Gastroenterology* **99:**1727–1735 (1990).
31. Chomczynski, P., and N. Sacchi. Single-step method of RNA isolation by acid guanidinium thiocyanate-phenol-chloroform extraction. *Anal. Biochem.* **162:**156–159 (1987).
32. Schmiedlin-Ren, P., P. E. Benedict, W. O. III Dobbins, M. Ghosh, J. C. Kolars, and P. B. Watkins. Cultured adult rat jejunal explants as a model for studying regulation of CYP3A. *Biochem. Pharmacol.* **46:**905–918 (1993).
33. Kolars, J. C., K. S. Lown, P. Schmiedlin-Ren, M. Ghosh, C. Fang, S. A. Wrighton, R. M. Merion, and P. B. Watkins. CYP3A gene expression in human gut epithelium. *Pharmacogenetics* **4:**247–259 (1994).
34. Chen, C., D. Clark, K. Ueda, I. Pastan, M. M. Gottesman, and I. B. Roninson. Genomic organization of the human multidrug resistance (MDR1) gene and origin of P-glycoproteins. *J. Biol. Chem.* **265:**506–514 (1990).
35. Sweetser, D. A., E. H. Birkenmeier, I. J. Klisak, S. Zollman, R. S. Sparkes, T. Mohandas, A. J. Lusis, and J. I. Gordon. The human and rodent intestinal fatty acid binding protein genes. *J. Biol. Chem.* **262:**16060–16071 (1987).
36. Arpin, M., E. Pringault, J. Finidori, A. Garcia, J.-M. Jeltsch, J. Vandekerckhove, and D. Louvard. Sequence of human villin: a large duplicated domain homologous with other actin-severing proteins and a unique small carboxy-terminal domain related to villin specificity. *J. Cell Biol.* **107:**1759–1766 (1988).
37. Pringault, E., S. Robine, and D. Louvard. Structure of the human villin gene. *Proc. Natl. Acad. Sci. USA* **88:**10811–10815 (1991).
38. Hashimoto, H., K. Toide, R. Kitamura, M. Fujita, S. Tagawa, S. Itoh, and T. Kamataki. Gene structure of CYP3A4, an adult-specific form of cytochrome P450 in human livers, and its transcriptional control. *Eur. J. Biochem.* **218:**585–595 (1993).
39. Itoh, S., T. Yanagimoto, S. Tagawa, H. Hashimoto, R. Kitamura, Y. Nakajima, T. Okochi, S. Fujimoto, J. Uchino, and T. Kamataki. Genomic organization of human fetal specific P-450 IIIA7 (cytochrome P-450HFLa)-related gene(s) and interaction of transcriptional regulatory factor with its DNA element in the 5′ flanking region. *Biochim. Biophys. Acta* **1130:**133–138 (1992).
40. Sanger, F., S. Nicklen, and A. R. Coulson. DNA sequencing with chain-terminating inhibitors. *Proc. Natl. Acad. Sci. USA* **74:**5463–5467 (1977).
41. Becker-Andre, M., and K. Hahlbrock. Absolute mRNA quantification using the polymerase chain reaction (PCR): a novel approach by a PCR aided transcript titration assay (PATTY). *Nucleic Acids Res.* **17:**9437–9446 (1989).
42. Gilliland, G., S. Perrin, K. Blanchard, and H. F. Bunn. Analysis of cytokine mRNA and DNA: Detection and quantitation by competitive polymerase chain reaction. *Proc. Natl. Acad. Sci. USA* **87:**2725–2729 (1990).
43. Lowry, O. H., N. J. Rosebrough, A. L. Farr, and R. J. Randall. Protein measurement with the Folin phenol reagent. *J. Biol. Chem.* **193:**265–275 (1951).
44. Nelson, D. R., L. Koymans, T. Kamataki, J. J. Stegeman, R. Feyereisen, D. J. Waxman, M. R. Waterman, O. Gotoh, M. J. Coon, R. W. Estabrook, I. C. Gunsalus, and D. W. Nebert. P450 superfamily: update on new sequences, gene mapping, accession numbers and nomenclature. *Pharmacogenetics* **6:**1–42 (1996).
45. Kronbach, T., D. Mathys, M. Umeno, F. J. Gonzalez, and U. A. Meyer. Oxidation of midazolam and triazolam by human liver cytochrome P450IIIA4. *Mol. Pharmacol.* **36:**89–96 (1989).
46. Wacher, V. J., C.-Y. Wu, and L. Z. Benet. Overlapping substrate specificities and tissue distribution of cytochrome P450 3A and P-glycoprotein: implications for drug delivery and activity in cancer chemotherapy. *Mol. Carcinog.* **13:**129–134 (1995).
47. Schuetz, E. G., W. T. Beck, and J. D. Schuetz. Modulators and substrates of P-glycoprotein and cytochrome P4503A coordinately up-regulate these proteins in human colon carcinoma cells. *Mol. Pharmacol.* **49:**311–318 (1996).
48. Halline, A. G., N. O. Davidson, S. F. Skarosi, M. D. Sitrin, C. Tietze, D. H. Alpers, and T. A. Brasitus. Effects of 1,25-dihydroxyvitamin D3 on proliferation and differentiation of Caco-2 cells. *Endocrinology* **134:**1710–1717 (1994).
49. Gorski, J. C., S. D. Hall, D. R. Jones, M. Vandenbranden, and S. A. Wrighton. Regioselective biotransformation of midazolam by members of the human P450 3A (CYP3A) subfamily. *Biochem. Pharmacol.* **47:**1643–1653 (1994).
50. Schuetz, J. D., and E. G. Schuetz. Extracellular matrix regulation of multidrug resistance in primary monolayer cultures of adult rat hepatocytes. *Cell Growth Differ.* **4:**31–40 (1993).
51. Prueksaritanont, T., L. M. Gorham, J. H. Hochman, L. O. Tran, and K. P. Vyas. Comparative studies of drug-metabolizing enzymes in dog, monkey, and human small intestines, and in Caco-2 cells. *Drug Metab. Dispos.* **24:**634–642 (1996).
52. Levin, M. S., V. D. Talkad, J. I. Gordon, and W. F. Stenson. Trafficking of exogenous fatty acids within Caco-2 cells. *J. Lipid Res.* **33:**9–19 (1992).
53. Walters, M. W. Newly identified actions of the vitamin D endocrine system. *Endocr. Rev.* **13:**719–764 (1992).
54. Norman, A. W., I. Nemere, L.-X. Zhou, J. E. Bishop, K. E. Lowe, A. C. Maiyar, E. D. Collins, T. Taoka, I. Sergeev, and M. C. Farach-Carson. $1,25(OH)_2$-Vitamin D_3, a steroid hormone that produces biologic effects via both genomic and nongenomic pathways. *J. Steroid Biochem. Mol. Biol.* **41:**231–240 (1992).
55. Adams, J. C., and F. M. Watt. Regulation of development and differentiation by the extracellular matrix. *Development* **117:**1183–1198 (1993).
56. Basson, M. D., G. Turowski, and N. J. Emenaker. Regulation of human (Caco-2) intestinal epithelial cell differentiation by extracellular matrix proteins. *Exp. Cell Res.* **225:**301–305 (1996).
57. Wagner, R. D., E. S. Krul, J. B. Moberly, D. H. Alpers, and G. Schonfeld. Apolipoprotein expression and cellular differentiation in Caco-2 intestinal cells. *Am. J. Physiol.* **263** (2 Part 1) **:**E374–E382 (1992).
58. Giuliano, A. R., R. T. Franceschi, and R. J. Wood. Characterization of the vitamin D receptor from the Caco-2 human colon carcinoma cell line: effect of cellular differentiation. *Arch. Biochem. Biophys.* **285:**261–269 (1991).
59. Chen, K.-S., and H. F. DeLuca. Cloning of the human 1*alpha*,25-dihydroxyvitamin D-3 24-hydroxylase gene promoter and identification of two vitamin D-responsive elements. *Biochim. Biophys. Acta* **1263:**1–9 (1995).
60. Ozono, K., J. Liao, S. A. Kerner, R. A. Scott, and J. W. Pike. The vitamin D-responsive element in the human osteocalcin gene. *J. Biol. Chem.* **265:**21881–21888 (1990).
61. Kerner, S. A., R. A. Scott, and J. W. Pike. Sequence elements in the human osteocalcin gene confer basal activation and inducible response to hormonal vitamin D3. *Proc. Natl. Acad. Sci. USA* **86:**4455–4459 (1989).
62. Morrison, N. A., J. Shine, J.-C. Fragonas, V. Verkest, M. L. McMenemy, and J. A. Eisman. 1,25-Dihydroxyvitamin D-responsive element and glucocorticoid repression in the osteocalcin gene. *Science (Washington D. C.)* **246:**1158–1161 (1989).
63. Demay, M. B., M. S. Kiernan, H. F. DeLuca, and H. M. Kronenberg. Sequences in the human parathyroid gene that bind the 1,25-dihydroxyvitamin D3 receptor and mediate transcriptional repression in response to 1,25-dihydroxyvitamin D3. *Proc. Natl. Acad. Sci. USA* **89:**8097–8101 (1992).
64. Huss, J. M., S. I. Wang, A. Astrom, P. McQuiddy, and C. B. Kasper. Dexamethasone responsiveness of a major glucocorticoid-inducible CYP3A gene is mediated by elements unrelated to a glucocorticoid receptor binding motif. *Proc. Natl. Acad. Sci. USA* **93:**4666–4670 (1996).
65. Barwick, J. L., L. C. Quattrochi, A. S. Mills, C. Potenza, R. H. Tukey, and P. S. Guzelian. Trans-species gene transfer for analysis of glucocorticoid-inducible transcriptional activation of transiently expressed human CYP3A4 and rabbit CYP3A6 in primary cultures of adult rat and rabbit hepatocytes. *Mol. Pharmacol.* **50:**10–16 (1996).
66. Deleted in proof.
67. Collington, G. K., J. Hunter, C. N. Allen, N. L. Simmons, and B. H. Hirst. Polarized efflux of 2′,7′-bis(2-carboxyethyl)-5(6)-carboxyfluorescein from cultured epithelial cell monolayers. *Biochem. Pharmacol.* **44:**417–424 (1992).
68. Pichard, L., I. Fabre, G. Fabre, J. Domergue, B. Saint Aubert, G. Mourad, and P. Maurel. Cyclosporin A drug interactions: screening for inducers and inhibitors of cytochrome P-450 (cyclosporin A oxidase) in primary cultures of human hepatocytes and in liver microsomes. *Drug Metab. Dispos.* **18:**595–606 (1990).
69. Holmans, P. L., M. S. Shet, C. A. Martin-Wixtrom, C. W. Fisher, and R. W. Estabrook. The high-level expression in *Escherichia coli* of the membrane-bound form of human and rat cytochrome b5 and studies on their mechanism and function. *Arch. Biochem. Biophys.* **312:**554–565 (1994).
70. Vergeres, G., and L. Waskell. Expression of cytochrome b5 in yeast and characterization of mutants of the membrane-anchoring domain. *J. Biol. Chem.* **267:**12583–12591 (1992).

Send reprint requests to: Paul B. Watkins, M.D., University of Michigan Medical Center, Room A7119 University Hospital, Box 0108, 1500 East Medical Center Drive, Ann Arbor, MI 48109. E-mail: pwatkins@umich.edu